Can biocrust moss hide from climate change? Multiscale habitat buffering improves summer-stress resistance in *Syntrichia caninervis*

Theresa A. Clark[1,2,3], Alexander Russell[1], Joshua L. Greenwood[1], Dale Devitt[1], Daniel Stanton[2], Lloyd R. Stark[1]

[1]School of Life Sciences, University of Nevada, Las Vegas, NV
[2]Department of Evolution, Ecology & Behavior, University of Minnesota, Twin Cities, MN
[3]Corresponding author

ABSTRACT

Premise: Dryland mosses provide many ecosystem functions but are the most vulnerable of biocrust organisms to climate change due to sensitive water relations particularly stressed by summer aridity. However, potential mitigating roles of habitat buffering on moss aridity exposure and stress resistance remain largely unexplored. We predicted the most buffered and healthiest biocrust mosses would occur in high-elevation forests on north-facing slopes beneath shrub canopies in the Mojave Desert.

Methods: We located three life zone populations of a keystone biocrust moss, *Syntrichia caninervis*, spanning 1200-m of altitude in Nevada. We selected 96 microsites stratified by life zone and topography zone (aspect and hydrological position), and microhabitat type (shrub proximity). We quantified end-of-summer photosynthetic stress (F_v/F_m), and aridity at three scales: macroclimate, mesoscale exposure, and microscale shade time.

Results: Moss habitat structure varied greatly across scales, revealing exposed and buffered microsites in all life zones. Moss stress did not differ by life zone despite the extensive macroclimate gradient but was lowest on N-facing slopes and microhabitats with higher shade, while the importance and interactions of topography, exposure, and shade varied by life zone.

Conclusions: Our findings support an emerging vulnerability paradigm for small dryland organisms: microrefugia may be more important than high-elevation macrorefugia for increasing resistance to climate stress. We demonstrate, for the first time, that multiple scales of interacting habitat structure appear to create physiologically significant buffered habitats for *S. caninervis*, which may allow this species to hide from the brunt of climate change in widespread microrefugia.

Keywords: biological soil crust; chlorophyll fluorescence; climate change; desert bryophytes; desiccation tolerance; habitat buffering; Mojave Desert; NevCAN; Syntrichia caninervis; water relations

semiarid environments globally (Belnap 2003). Where sufficient moisture exists, mosses are often the larger members of these soil communities and drive many biocrust ecosystem services (Bowker et al. 2013) mediated by their large (typically 1 – 10 cm^2), absorbent colonies or "patches" that can increase water infiltration and retention (Lafuente et al. 2018), buffer temperature (Xiao et al. 2015), increase soil fertility (Belnap 2003), shelter microbiota (Abed et al. 2019, Fisher et al. 2020), store carbon (Elbert et al. 2012), and prevent erosion (Stovall et al. 2022). However, biocrust mosses are predicted to have more dramatic responses to climate change than most other poikilohydric biocrust species because of their requirements for higher shade and moisture during hydration periods (i.e., "hydroperiods") when the plants are metabolically active (He et al. 2016, Rodriguez-Caballero et al. 2018, Weber et al. 2018, Ladrón de Guevara & Maestre 2022).

Habitat buffering may shelter biocrust mosses from climatic extremes

The habitat buffering hypothesis predicts that sheltered microhabitats will reduce climate stress for many organisms (Williams et al. 2008, Scheffers et al. 2013, Shi et al. 2016). Despite the prevalence of topographically complex, multiscaled biocrust environments (e.g., Williams et al. 2013, Pietrasiak et al. 2014, Bowker et al. 2016), no research has assessed patterns in biocrust moss stress and mortality in relation to multiscaled habitat structure and its potential habitat buffering gradients. To our knowledge, it has been suggested but not confirmed that high-elevation habitat (e.g. mountains), north-facing slopes (in the northern hemisphere), and shade vegetation may offer an oasis to dryland mosses by reducing local extremes in temperature, incident radiation, and evaporative demand (He et al. 2016, Li et al. 2018, Ladrón de Guevara & Maestre 2022). Aridity is known to drive patterns in moss abundance and community composition in many drylands (Nash et al. 1977, Seppelt et al. 2016, Clark 2020), however no studies have tested the physiological significance and prevalence of biocrust moss habitat buffering over natural, multiscaled aridity gradients.

We propose that measuring climatically sensitive biometrics, such as photosynthetic stress (i.e. measured by chlorophyll fluorescence or gas exchange analysis), in relation to habitat buffering will strengthen current predictions for future moss distributions in drylands (Coe & Sparks 2014). We propose that combining stress measures into a multiscale habitat framework that addresses the spatial scales relevant to biocrust mosses (Bowker et al. 2006) will further strengthen vulnerability predictions by elucidating the types of refugia (i.e. macro- or microrefugia; Ashcroft 2010) that may exist for these small photosynthetic organisms. To this end, we hypothesized that habitat buffering of moss biocrust operates at multiple potentially interacting scales of habitat structure relevant to their small patch size, often less than 5 cm^2 (Nash et al. 1977, Clark 2020). If ecophysiologically significant buffered habitats exist for biocrust, these microsites should support increased stress resistance, growth, and reproduction in resident moss patches.

Model system and keystone biocrust moss in the Mojave Desert

Syntrichia caninervis Mitten, a member of the acrocarpous moss family, Pottiaceae, is a keystone biocrust species understood to be one of the most broadly distributed and ecologically important biocrust mosses in the world; the species forms variously sized, scattered patches in biocrusts of North America, North Africa, and Asia (e.g., Maestre et al. 2012, Seppelt et al. 2016, Ros et al. 1999, Zhang & Zhang 2020). Thirteen years have passed

since the last climate stress assessment for *S. caninervis* in the American Southwest (Belnap et al. 2004, Barker et al. 2005) while ecophysiological models predict climatic limitations on the species' carbon balance will greatly reduce its future productivity by 25 – 63% while increasing mortality (Coe and Sparks 2014). Moreover, multiple field and laboratory experiments simulating extreme climate stress (e.g., rapid drying events) have caused severe tissue damage or lethality in this species (e.g. Brinda et al. 2011, Stark et al. 2011, Reed et al. 2012, Zhang et al. 2016b, Coe et al. 2020) further suggesting *S. caninervis* may be threatened by continued climate change.

Current climate trends and predictions in this most arid North American desert include smaller summer rain events and increased drought intensity and variability (Seager & Vecchi 2010). Summer presents the highest risk for moss mortality when combinations of extreme desiccation (i.e., cellular water potentials < -400 mPa) interrupted by small rain events have been shown to prevent *S. caninervis* from achieving positive carbon balance during summer hydroperiods (Coe et al. 2012b). With a broad geographical and altitudinal distribution in the American Southwest (BFNA 2007), *S. caninervis* provides an ideal model species to study summer stress resistance along multiscaled gradients in habitat structure. The Mojave Desert is the most climatically extreme part the species' North American range where resident populations likely exist at or near physiological thresholds of precipitation minima and temperature maxima (e.g. Stark et al. 2009)**.** However, we know little about niche variation in aridity exposure, habitat structure, and potential habitat buffering in this desert moss.

Objectives

To this end, we sought to improve the vulnerability assessment of Mojave moss biocrust to future climate change in the Mojave Desert ecoregion by studying along a ~2000-m elevation-life zone gradient in the Desert National Wildlife Refuge (DNWR), Nevada to: (1) delineate aridity exposure of *S. caninervis* by determining its elevational and habitat distribution across three nested scales of habitat structure in the DNWR (life zone, topographical exposure, and microhabitat exposure), (2) determine how this habitat structure shapes moss shade buffering using our novel moss-scaled metric, annual shade time, (3) use chlorophyll fluorescence of moss patches to measure end-of-summer moss photosynthetic stress and mortality, if present, (4) explore the physiological importance of habitat structure and buffering to biocrust moss by testing if multiscale habitat structure and buffering proxies (macroclimate, potential insolation, and shade) are related to summer stress in *S. caninervis*.

Regarding (3) and (4) above, we hypothesized moss stress would increase with aridity exposure across each of the three scales of habitat structure, and thus, stress would be inversely related to elevation-life zone (i.e., cooler and wetter climate at higher elevations will be less stressful), topographical exposure (i.e., North-facing microsites will be less stressful than South-facing or flat microsites), and microhabitat exposure (i.e., microsites under shrubs will be less stressful than interspaces between shrubs). Our multiscale hypothesis would predict (1) lowest stress and least mortality will occur at the highest-elevation life zone on northerly-facing slopes, under shrub canopies offering greatest annual shade time, and (2) highest stress and most mortality will occur at the lowest-elevation life zone on southerly-facing slopes in the least-shaded interspace microhabitats.

MATERIALS AND METHODS

Life zone sites

The Desert National Wildlife Refuge (DNWR) is a large (6,430 km^2) topographically and biologically diverse basin and range landscape in the eastern Mojave Desert of southern Nevada. DNWR is home to the Sheep Range EPSCoR-NevCAN transect (*Established Program to Stimulate Competitive Research - Nevada Ecohydrological Climate Assessment Network;* Mensing et al. 2013), a set of five climate stations spanning 2000 m of elevation and located in one of the five Mojave life zones (**Fig. 1a**), all of which have been floristically characterized without mention of bryophytes (Ackerman 2003, NCCP 2018). Regional soils are limestone-derived, highly calcareous, and range from low-organic to relatively high organic content at high elevations.

The lowest elevation desert scrubland site (890 m, N36.435345, W115.355850; "Low-scrubland") and surrounding landscape are characterized by an open salt basin interrupted by shallow, calcareous drainages with gentle slopes and occasional steep ravines 1 – 2 m deep. Excluding drainages, the soil is covered almost entirely by desert pavement (e.g. Pietrasiak et al. 2014) with well-spaced shrubs (>2 m apart) and (**Fig. 2a**). The blackbrush-Joshua tree (*Coleogyne ramosissima and Yucca brevifolia*) life zone site (1680 m, N36.51723, W115.16191; "Mid-shrubland") is situated in the center of an intermountain basin divided by drainages that range from ~1 – 3 m deep. The ground is nearly covered by desert pavement, moderately spaced shrubs (<2 m apart), and widely spaced succulents (**Fig. 2a**). The pinyon-juniper woodland site (2065 m, N36.572808, W115.204060; "High-woodland") is at the base of the Sheep Mountains on one of the deeply divided ridges with steep, rocky slopes (>3 m tall, ~10° - 15°). The soil is nearly covered by loose gravel with a dense community of short and tall shrubs and the dominant well-spaced pygmy conifers (*Pinus monophyla* and *Juniperus osteosperma*; **Fig. 2a**). The Montane site (2320 m, N36.590255, W115.214166) has an open-canopy of *Pinus ponderosa* and well-spaced shrubs (>3m apart). The highest-elevation Subalpine site (3015 m, N36.657641 W115.200777) in the NevCAN transect is a nearly closed-canopy mixed-conifer forest (*Abies* concolor, *A. lasiocarpa*, *Picea englemannii*, and *Pinus longaeva*) with calcareous, rocky, organic soils (Ackerman 2003).

Climate metrics

To compare mean annual and summer climate where we located *S. caninervis* along the NevCAN-DNWR life zone transect, we acquired NevCAN daily means for temperature, humidity, irradiance, and precipitation from 2011 – 2018 (DRI, 2020). We calculated the 7-yr mean annual air and soil temperature, percent relative humidity (RH), wind speed, and soil moisture. We calculated summer 2017 climate means to include Mojave hot-season months preceding our moss tissue collection, which took place at the beginning of November (6/1/17 – 11/6/17; **Table 1a**).

Aridity exposure survey: life zones, topography zones, & microhabitats

To determine the macroclimate exposure of *S. caninervis* in DNWR across the three habitat gradients, we surveyed for species occurrence within a 1-km radius of each life zone climate tower (**Fig. 1a & b**); when we found the species in a life zone, we surveyed three topographical exposure zones (40 x 10 m plots) selecting the most northerly-facing, southerly-

Table 1. Habitat buffering on three scales (life zones, topography zones, & microhabitats)

Table 1. Macroclimate measured by the NevCAN station near each life zone study site supporting *S. caninervis* in DNWR. **(a)** Annual (2011 – 2018) and Summer (6/1/17 – 11/6/17) daily climate means ± (SD). The maximum life zone buffer (**Mean buffer**) is the maximum deviance between the three life-zone means for the respective period. **(b)** Mean ± (SD) potential direct incident radiation (***Mean PDIR***) for life zone sites and topography zones (see **Fig. 1**). The greatest topography zone buffer (**Mean buffer**) is the greatest mean deviance between all pairwise comparisons between topography zones for each row. Topography zones varied in their sample sizes (see Fig. 1c); SD = 0 occurred on two topography zones having nearly identical exposure across microsites.

		Life zone site				
		All sites	Low-scrubland (creosote, 890 m)	Mid-shrubland (blackbrush, 1670 m)	High-woodland (pinyon-juniper, 2070 m)	
a) Climate metric		**Mean (SD)**				**Mean buffer**
Air temperature (°C)	Annual	15.0 (9)	18.9 (9)	13.8 (8)	12.3 (8)	(-) 6.6 °C
	Summer	22.6 (6)	26.9 (6)	21.3 (6)	19.5 (6)	(-) 7.4 °C
Soil temperature (°C)	Annual	17.3 (11)	21.8 (11)	16.2 (10)	13.9 (10)	(-) 7.9 °C
	Summer	26.0 (7)	31.1 (7)	24.9 (7)	22.1 (6)	(-) 9.0 °C
Relative Humidity (%)	Annual	32 (19)	29 (17)	34 (19)	35 (20)	(+) 6%
	Summer	26 (13)	21 (11)	28 (14)	29 (15)	(+) 8%
Wind Speed (m/s)	Annual	3.6 (1)	4.2 (2)	3.8 (1)	2.8 (1)	(-) 1.4 m/s
	Summer	3.6 (1)	4.2 (1)	3.8 (1)	2.8 (1)	(-) 1.4 m/s
Soil moisture (θ)	Annual	6.1 (6)	2.9 (4)	5.8 (6)	14.5 (5)	(+) 11.6 θ
Precipitation (mm)[2]	Annual	186 (52)	119 (41)	160 (54)	278 (85)	(+) 159 mm/yr
	Summer[2]	92	26	81	169	(+) 143 mm
b) Topography zone		**Mean PDIR (kJ/cm²/yr)**				**Mean buffer**
Topography zones pooled		943	905	975	949	(-) 70 kJ/cm²/yr
South-facing zone[1]		1022[1]	1061[1]	999 (8)	1044 (4)	(-) 45 kJ/cm²/yr
Flat terrain zone		990	985 (0)	1000 (0)	986 (2)	(-) 15 kJ/cm²/yr
North-facing zone		856	826 (16)	926 (8)	817 (29)	(-) 109 kJ/cm²/yr

Notes: Climate metrics were measured at 2-m height except for soil temperature and moisture, measured at 1 and 4 inches subsurface, respectively. [1]The S-facing slope at the Low-scrubland site was not included in mean calculations because no mosses were found there. [2]The standard deviation of total precipitation is annual variability, and thus summer 2017 total precipitation has no standard deviation.

Figure 1. Distribution survey & sampling of populations across nested habitat gradients

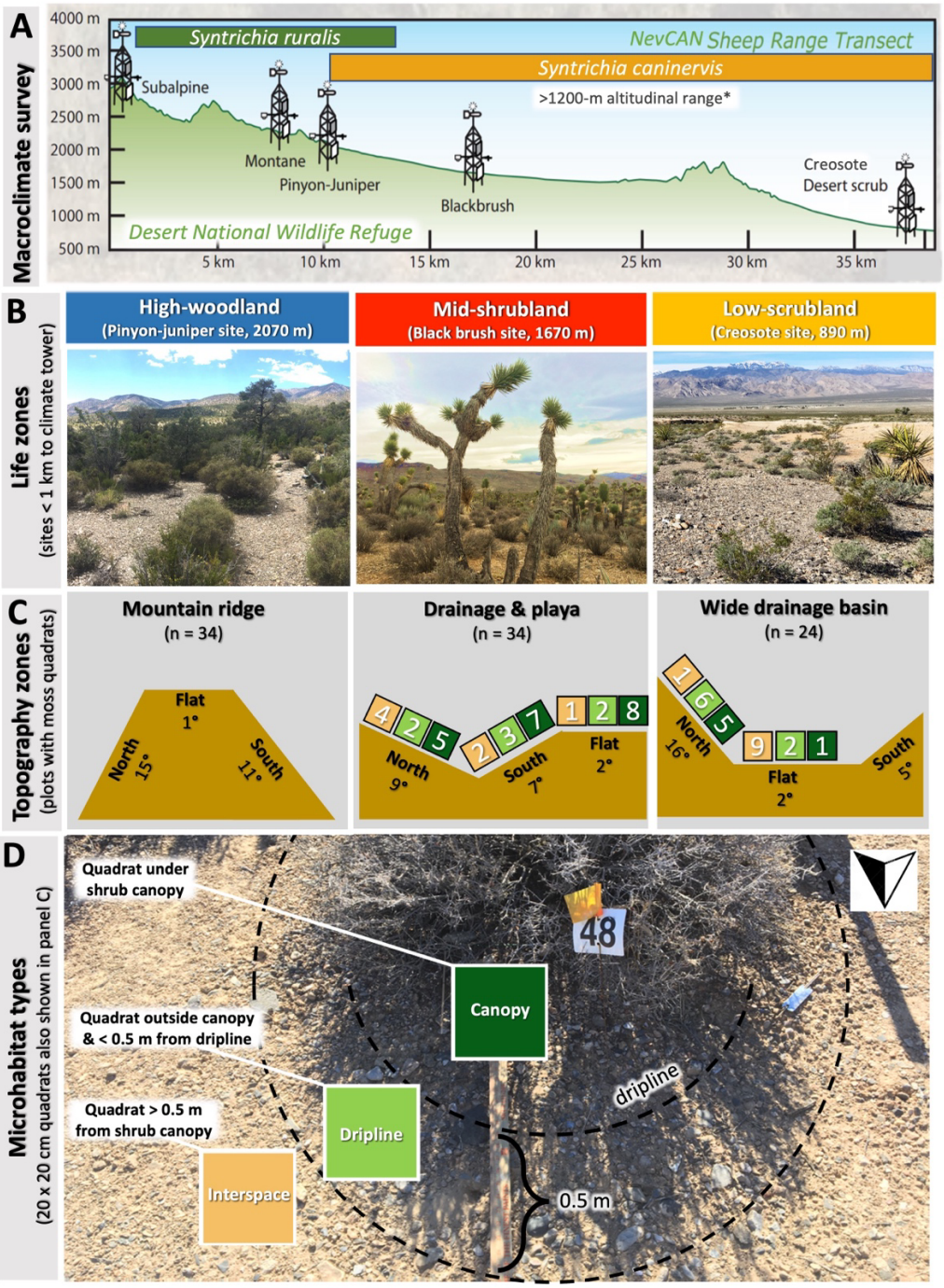

Figure 1. A. Elevation range surveyed for *S. caninervis* in the Sheep Range of the Mojave Desert National Wildlife Refuge (DNWR). EPSCoR-NevCAN climate towers are shown in each life zone (see text). Final sample of 92 microsites (20 x 20 cm quadrats enumerated in **C**) spanned three aridity exposure gradients: life zones (**B**), topography zones (northerly, southerly, or flat transects, **C**), and microhabitat shade types (**D**). For each topography zone in **C**, the slope and microhabitat frequency are shown and missing squares indicate *S. caninervis* was not found for a given zone or microhabitat type. See **Figure 3** for example quadrats.

facing, and flat terrain nearest the tower. Selected topography zones varied in their hydrological positions, including association with drainages, uplands, or mountain ridges (**Fig. 1c**). Within each topography zone, we surveyed for moss occurrence in three microhabitat shade classes (called "*microhabitat types*" hereafter): (1) high-exposure *interspace habitats* (≥ 0.5 m from the shrub dripline), (2) low-exposure *canopy habitats* (partially or fully under shrub canopies), and (3) intermediate-exposure *dripline habitats* located in the shrub dripline (i.e., within a narrow margin outside the shrub canopy but within 0.5 m of the dripline; **Fig. 1 d**). Any vegetation located to the north (cardinal 315° – 45°) of moss microsites was ignored in habitat type assignment because it did not contribute to moss shade.

Moss microsite selection – We systematically selected 12 microsites per topography zone, attempting to find 4 of each microhabitat type per topography zone, but because this was often not possible (see **Fig. 1c**), the resulting proportion of microhabitats at each life zone is a coarse measure of habitat frequency (**S1**). We selected only undisturbed microhabitats having the shrub canopy intact (i.e., not dead or broken off). We systematically centered a 20 x 20 cm quadrat over the highest-density patch of *S. caninervis* in each microhabitat (>3 cm^2 of *S. caninervis* cover), orienting the quadrat with sides parallel to a North-South axis (**Fig. 1d**). Four shoots were sampled from each quadrat for microscopic species verification; however, mid-way in the study, we removed two microsites after finding (via lab culture) two *Syntrichia* species (*caninervis* and *ruralis* sensu lato) were unknowingly intermixed and possibly measured in the stress assay (Clark 2020; **Fig. 1a**).

Habitat buffering metrics

We used three habitat buffering proxies, one for each scale of habitat structure, based on continuous (rather than categorical) abiotic habitat variables. "Habitat buffering" implies environmental variation in the direction of conditions more favorable to, in this case, mosses (e.g., increasing humidity, decreasing temperature and insolation). The use of buffering proxies rather absolute changes in climate – measured via microclimate sensors – is more practical for studying large samples of moss microsites (~100) while also being a less invasive method in delicate biocrust systems.

Macroscale climate buffering – Life zone buffering was estimated at the landscape scale by calculating the mean difference in macroclimate relative to the low-elevation Creosote life zone where conditions are most stressful for mosses (i.e. most arid and hot). For example, the life zone temperature buffer was calculated as the mean annual decrease in daily temperature between the creosote life zone and the higher life zones.

Mesoscale topographical buffering – We measured aspect (compass cardinal direction) and slope (Suunto PM-5 hand-held clinometer) of the 3 x 3 m^2 area surrounding each microsite for use in calculating potential direct incident radiation (PDIR). Within life zones, we calculated mesoscale topographical exposure as the mean of microsite PDIR in each topography zone. PDIR was estimated with a complex formula that incorporates microsite elevation, latitude, slope, and folded aspect (McCune & Keon 2002, McCune 2007). We folded aspect along a N – S axis (rather than NE-SW) because we observed *S. caninervis* ground cover to be greatest on the N rather than NE side of shrubs suggesting that N to S was the strongest exposure gradient for mosses in this ecosystem. Therefore, folded aspect transformed each azimuth (*A*) to a decimal from 0° to 180°, mirroring the N – S axis by the equation, $180° - |180° - A°|$. We then calculated

various topography zone buffers (e.g. the maximum buffer is simply the difference of the topography zone with the highest mean PDIR minus that with the lowest mean PDIR).

Microscale shade buffering – To precisely measure fine-scale shade time of microsites, we developed a photographic method using the smartphone app, *Sun Seeker© Solar AR (Augmented Reality) Tracker* (Sydney, Australia), which maps onto the camera view the annual solar window from sunset to sunrise for a given location (e.g., moss microsite). Seven photos taken at any time of the year circumscribe all geographical-time-referenced shade objects from the vantage point of the moss (**Fig. 2**). For each photo, the area of shade objects (i.e., vegetation and topography) inside the solar window was scored using a shade class from 0 (no shade) to 4 (75 – 100% shaded; see classes in **Fig. 2**). For each microsite, the resulting seven shade classes were divided by the total possible score of 28 shade points to yield an annual shade time percentage. Our novel microscale shade metric estimates the percentage of the year a microhabitat is shaded by vegetation and/or topography; we used this sensor-free buffering metric to test differences in mean shade at various scales of habitat structure.

Field sampling & tissue prep

To measure the summer stress signal of *S. caninervis*, we collected shoots when patches were fully desiccated in late fall (November 6 – 13, 2017; *Permit #84555-17-019 U.S. Fish and Wildlife Service National Refuge System Research & Monitoring*). The dry tissue preserved the summer stress signal because we collected prior to any fall precipitation (**Fig. 3a**). We collected two to three shoots for every 2-cm^2 of patch area per quadrat using fine forceps. Collections were stored dark and dry at 20°C with 20 – 30% relative humidity, conditions which should not exacerbate stress in this species (Guo & Zhao 2018). Before the stress assay, shoots were hydrated with distilled water on a microscope slide and the upper 2 mm were cut and retained to target the living apical "green zone" (Stark 2017) (**Fig. 3b**). Green zones were swirled in a drop of water to remove debris, and placed vertically into a rosette formation on a wetted 7-mm filter paper disc creating a "*moss bouquet"* (**Fig. 3b**). The number of shoots in a moss bouquet (5 – 23) depended on shoot size to maximize microsite representation and standardize leaf area for chlorophyll fluorescence.

Summer-stress resistance assay (Fv/Fm)

Efficiency of photosystem II (PSII) photosynthesis is commonly measured in plants to assess stress via the non-invasive technique, chlorophyll fluorescence (Papadatos et al. 2017), convenient for measurements on small moss species with limited biomass or long-term monitoring (Proctor 2009). Our stress measurements were performed with a Hansatech FMS-2 modulated fluorometer (Norfolk, England) and modified leaf clips hollowed to accommodate taller shoots (**Fig. 3b & c**). Hydrated moss bouquets were each placed on a folded chemical-wipe and carefully positioned into leaf clips, then placed in a tray of distilled water to maintain full-turgor throughout the 20-min dark adaptation (a period needed to close all active PSII reaction centers). Including 10 min to clean and prep bouquets, we measured chlorophyll fluorescence at 30-min post-rehydration, a standard photosynthetic reactivation timepoint for assessing the 'photosynthetic stress' or 'vitality' of mosses prior to significant recovery from the preceding desiccation event (e.g., Munzi et al. 2019, Hamerlynck et al. 2000, Ekwealor et al. 2021).

Figure 2. Sun Seeker© shade time method

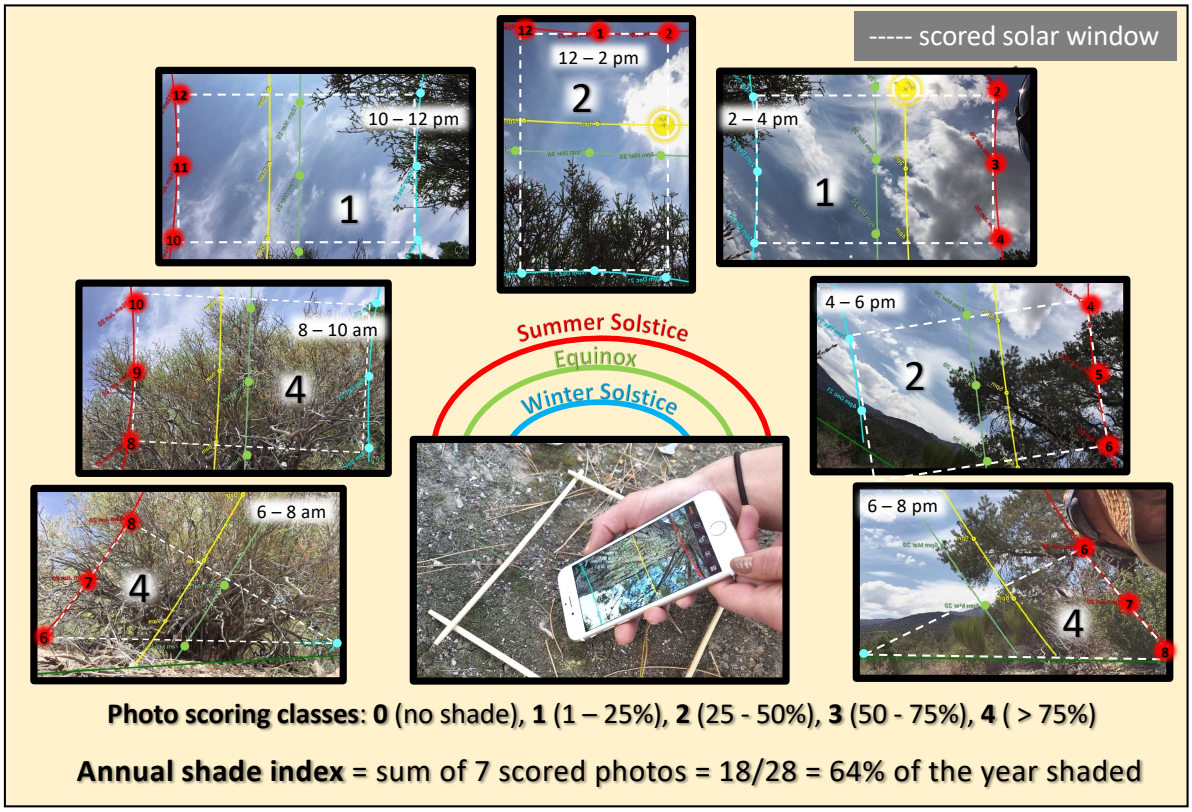

Figure 2. Microsite annual shade time was quantified using seven photos taken on a smartphone using the *Sun Seeker© Solar AR Tracker* app. The phone was held approximately 1 cm above the center of each microsite quadrat (***center photo***) and the photos encompass the solar arc from 6 am to 8 pm (***red circles***), which collectively captures the annual solar window from summer solstice (***red lines***) to winter solstice (blue lines) for a single microsite. Photos are scored using a 5-scale percent shade class by assessing the area of all shade objects intersecting each 2-h solar window (***white dashed boxes and triangles***). Percent annual shade time is the sum of classes for all seven photos divided by 28, the maximum possible (i.e. for a habitat shaded 75-100% of the year). The microsite shown here is shaded 64% of the year ((4 + 4 + 1 + 2 + 1 + 2 + 4 = 18)/28 = 0.64 x 100). Note: the center photo in this figure showing the smartphone position is not located at the microsite of the illustrated solar window.

Figure 3. Sampling and stress assay methods for small biocrust moss

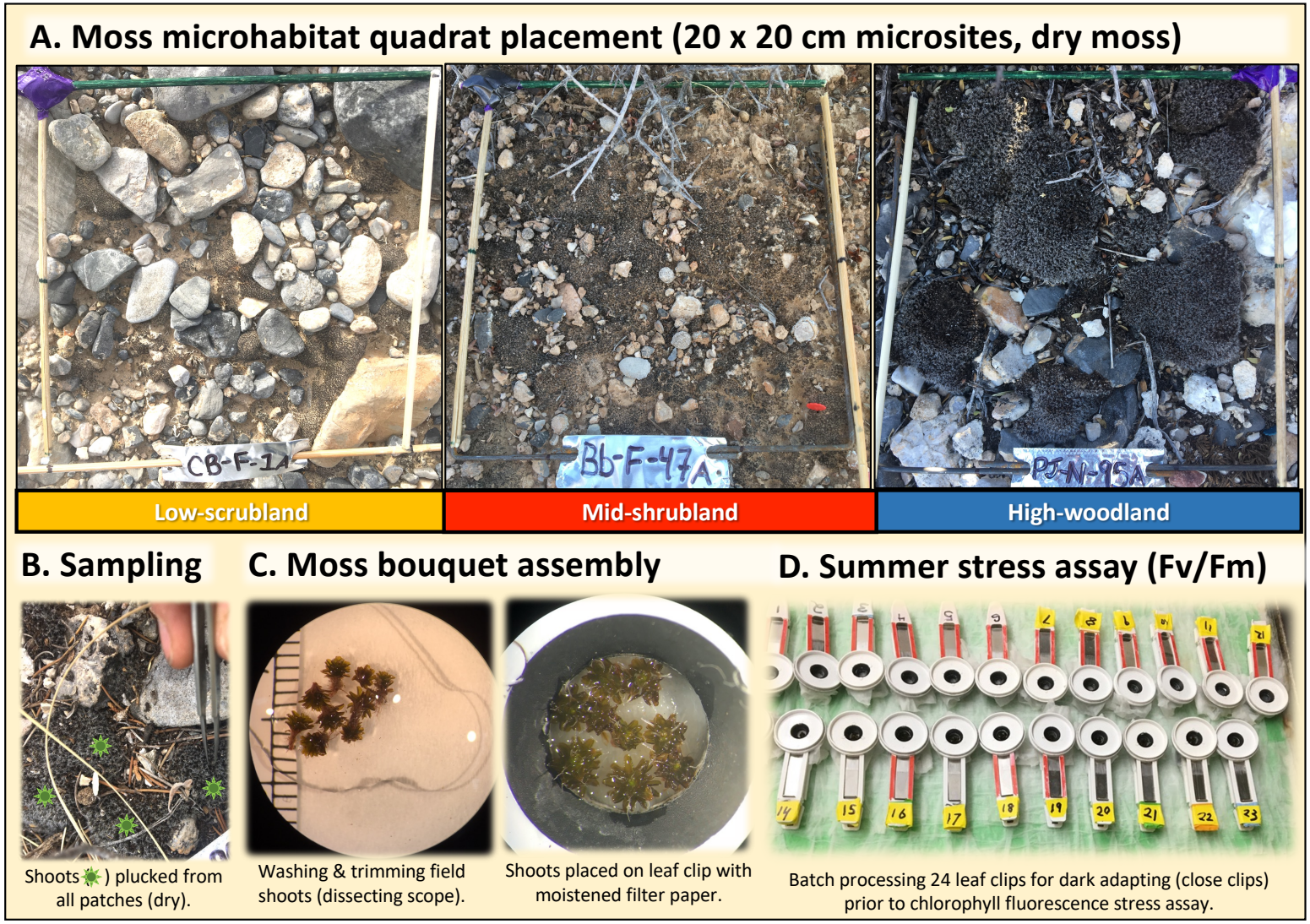

Figure 3. Methods for microhabitat selection at three life zone sites showing moss abundance gradient (**A**), field shoot sampling (**B**), moss bouquet assembly (**C**), and the photosynthetic efficiency assay (**D**) to test summer stress in a small desert moss.

A Hansatech script automated our measurement of the dark-adapted metrics, basal (Fo) and maximum (Fm) fluorescence, during a 0.8-s saturation pulse of 3000 μmol/m^2/s. Using variable fluorescence (Fv = Fm – Fo), our stress proxy (Fv/Fm) was then derived, which estimates potential maximum quantum efficiency of photosystem II (PSII) photochemistry of dark-adapted plants (Baker 2008). Fv/Fm provides a universal physiological indicator of climate stress in plants that is more sensitive and integrative than chlorophyll content (Murchie & Lawson 2013) and requires less tissue and time than gas exchange analysis.

Analysis

Code and data availability – Analyses were performed in *R* (Version 1.447 and 4.2.3; R Core Team 2023) using the *tidyverse* package (Wickham et al. 2019) with details referenced herein as (*package::function*). We used an exploratory approach with hypothesis testing in which we consider the ecological significance of statistical patterns when *P* is < 0.05 and opt out of arbitrary family corrections for testing our small set of environmental factors (Gotelli and Ellison 2013). We aid our interpretation of patterns using plots of raw data, distributional shape, and central tendency (*ggplot2*; Wickham 2016) because all are needed to interpret important variation in stress ecophysiology (Amrhein et al. 2019).

Shade buffering & moss stress vs multiscale habitat structure – Although our design involved three categorical habitat predictors of moss stress and shade buffering (life zone, topography zone, and microhabitat type), using three-way ANOVA's to test patterns in mean shade buffering and moss stress were not possible due to missing factor levels (i.e. no S-facing zone in the Low-scrubland and no interspace microhabitats in several topography zones (**Fig. 1c, S1**). Alternatively, we conducted six univariate ANOVA's: three stress tests and three shade buffering tests, one for each habitat factor. We calculated the effect sizes, Eta-squared (equivalent to R^2 in one-way ANOVA) and Cohen's *f* (Lakens 2013) to facilitate comparisons across the family of tests. When heteroskedasticity was present (Fligner-Killeen test; *stats::fligner.test*; Fligner & Killeen 1976), we opted out of transformations, which are known to yield nonsensical predictions of proportion data and hinder interpretability (Warton and Hui 2011). Instead, we used robust Welch's denominator degrees of freedom corrections appropriate for the approximate normality, unbalanced design, and heteroskedasticity present (*stats::oneway.test(var.equal=FALSE)*; Welch 1951); post-hoc tests for the Welch's ANOVA's were nonparametric Games-Howell familywise multiple comparisons (*rstatix::games_howell_test*; Kassambara 2023, Games & Howell 1976, Ruxton & Beauchamp 2008).

Multiscale habitat buffering proxies as predictors of moss stress – To explore the relationship between the three scales of habitat buffering (elevation, PDIR, and shade) and summer stress, we fit a linear multiple regression model for Fv/Fm (**S2**). Despite small variance inflation factors of 2.07, 1.17, 2.19, for the three predictors, respectively, our model testing procedure revealed instability in parameter estimates and p-values when elevation was included in the model (and no interaction terms were included). Therefore, the final reduced model included only PDIR, shade, and their interaction, centering the explanatory variables to remove structural multicollinearity. Diagnostic residual plots revealed adequate fit (**S3**);

however, more complex beta regression is optimal for modeling such a two-category ratio (Douma & Weedon 2018) and should be used for prediction-focused studies.

Life zone models – With life zone management in mind, we performed a set of hypothesis tests focused on each life zone-site to explore whether our spatially efficient (i.e. nested) sampling design (**Fig. 1**) of meso-scale topography zones (within-site plots) and micro-scale shade measurements (within-plot microsite quadrats) could explain significant patterns in moss stress. (Note: although ideal, testing these relationships in a single ANOVA model including all life zones was not possible due to the multicollinearity between site (elevation) and shade (as discussed in the habitat buffering model above).

Alternatively, we ran three separate ANOVAs (i.e. ANCOVAs) to test additive and interactive relationships between topography zone and percent shade time (centered before analysis) with moss stress for each life zone. ANOVAs were made robust to (a) the unbalanced design (**Fig. 1c**) using Type II sums of squares (Langsrud 2003, Logan 2010) and to (b) unequal variance using a Huber-white heteroskedasticity-corrected covariance matrix (HCCM; White 1980; Long & Ervin 2000) for each model (*car::Anova(white.adjust =* 'hc3', type = 'II', Fox & Weisberg 2019). Post-hoc pairwise comparisons for regression slopes (by topography zone) were not conducted (when the interaction term was significant) because we believe sample sizes greater than 11 – 12 quadrats per topography zone should be collected to produce more accurate fine-scale relationships. The OLS coefficient of determination (R^2) is shown for each final model as an effect size metric; the overall F-test for each HCCM-corrected model was derived from a Wald test comparing the intercept model to the respective HCCM model including only significant terms (*lmtest::waldtest(vcov = 'hc3'*); Zeileis & Hothorn 2002).

RESULTS

We use the terms *sites* and *life zones* interchangeably throughout the results and discussion. Results are numbered by objective and statistics are printed in figures if not shown here. The photosynthetic stress metric, Fv/Fm, will also be called "stress" hereafter. We refer to our three scales of aridity gradient sampling (i.e., life zones, topography zones, and microhabitat types, **Fig. 1**) as the three scales of habitat structure or habitat buffering, depending on context.

Aridity exposure across life zones (Objective 1)

After extensive surveying within a 1-km radius of each NevCAN climate tower, we located *S. caninervis* biocrust in the lower three sites of the DNWR eco-hydrological gradient spanning 1,180 m of elevation from 890 to 2070 m, while a closely related species, *Syntrichia ruralis* sensu lato, was found primarily at higher elevations (**Fig. 1a**); we will refer to these sampling sites as the Low-scrubland, Mid-shrubland, and High-woodland, respectively (**Fig. 1b**). We located *S. caninervis* on North-facing, South-facing, and flat topography zones at the Mid-shrubland and High-woodland, but it was absent from southerly facing slopes at the Low-scrubland (also absent from upland flats) and was only found on shallow drainage flats and northerly-facing slopes (**Fig. 1c**). In the Low and Mid-elevation sites, *S. caninervis* occurred in all three microhabitat types, but in the High-woodland, shrub interspace habitat did not support high-density *S. caninervis*. Relative habitat frequency changed with elevation: shrub canopy habitat increased, interspace habitat decreased, and shrub-dripline frequency remained similar

from low to high elevation (**S1, Fig. 1c**). Supporting our hypothesis, canopy microhabitats were the most frequent habitat type supporting high-density *S. caninervis* biocrust across life zones (54/94 microsites, **S1**).

Habitat buffering across three scales of habitat structure (Objective 2)

Macroscale climate buffering – Mean daily macroclimate differed substantially by life zone (**Table 1a**) with higher elevations having cooler temperatures, higher humidity and precipitation, and slower wind speeds. Relative to the Low-scrubland, the High-woodland site was climatically buffered in four metrics: (1) 6.5 times more precipitation, (2) reduced mean daily air and soil temperatures by -7.4°C and -9.0°C, respectively, and (3) increased mean relative humidity by +8% (**Table 1a**).

Mesoscale topographical buffering – The nine topography zones collectively represent the mesoscale exposure gradient for *S. caninervis*-dominant biocrust at each site and varied in their hydrological position by life zone: the Low-scrubland site was in an ephemeral drainage, the Mid-shrubland included a drainage and upland flat, and the High-woodland traversed a mountain ridge (**Fig. 1c**). Of the nine topography zones, there was a 22% reduction from the highest mean PDIR of the S-facing slope of the High-woodland (1044 kJ/cm²/yr) to the lowest mean PDIR of the N-facing slope of the High-woodland (817 kJ/cm²/yr), which created a maximum mean topography zone buffer of 227 kJ/cm²/yr (**Table 1b, Fig. 1c**). Notably, the Low-scrubland had the lowest average PDIR (of 24 microsites) due to its relatively steep 16° N-facing slope.

Microscale shade buffering – Percent annual shade time ("shade" hereafter) across the 94 microsites ranged from 21 – 96% and averaged 64 ± 2% (SE) such that most microsites were shaded over half of the year. Life zone significantly explained 48% of shade variation ($^{Welch}F_{2, 52}$ = 40.6, P < 0.0001); mean shade in the High-woodland was 1.9x greater than in the Low-scrubland (**Fig. 4a**). Mean shade differed little by topography zone when pooling microsites across life zones ($^{Welch}F_{2, 58}$ = 2.7, P = 0.074, R^2 = 0.05, **Fig. 4b**), while microhabitat type explained 67% of variation in shade, which increased 2.5-fold from interspace to canopy habitats, on average ($^{Welch}F_{2, 44} = 44.0$, P < 0.0001, **Fig. 4c**).

Summer stress by life zone (Objective 3)

The visual appearance of *S. caninervis* patches at the end of summer ranged from obviously damaged shoots with reddish-orange leaf tips to those lacking visible damage but darkly sun-pigmented (**Fig. 5**) such that chlorophyll fluorescence revealed a much larger variation in photosynthetic summer stress than could be detected visually. The sample distribution of stress was left-skewed with a mean Fv/Fm of 0.455 ± 0.148 (SE) and ranged from a severely stressed moss at 0.130 (i.e. potentially near death) at the Mid-shrubland to healthy moss at 0.737 at the Mid-shrubland (**Fig. 6**). Of the 94 mosses, ~23% were healthy (Fv/Fm >0.6) leaving 77% stressed. Dividing the typical physiological range of Fv/Fm (0 – 0.85) into four stress categories, we report 7% severely stressed, 25% moderately stressed, and 42% mildly stressed, and 26% unstressed (**Fig. 6**). Over 50% of the field samples had a moderate to extreme photosynthetic stress signal with severely stressed individuals present at all three life zones (**Fig. 6**).

Contradicting our hypothesis, southerly-facing topography zones did not support the most stressed mosses. In contrast, the seven most summer-stressed samples with Fv/Fm < 0.2

Figure 4. Shade buffering & moss stress across three scales of habitat structure.

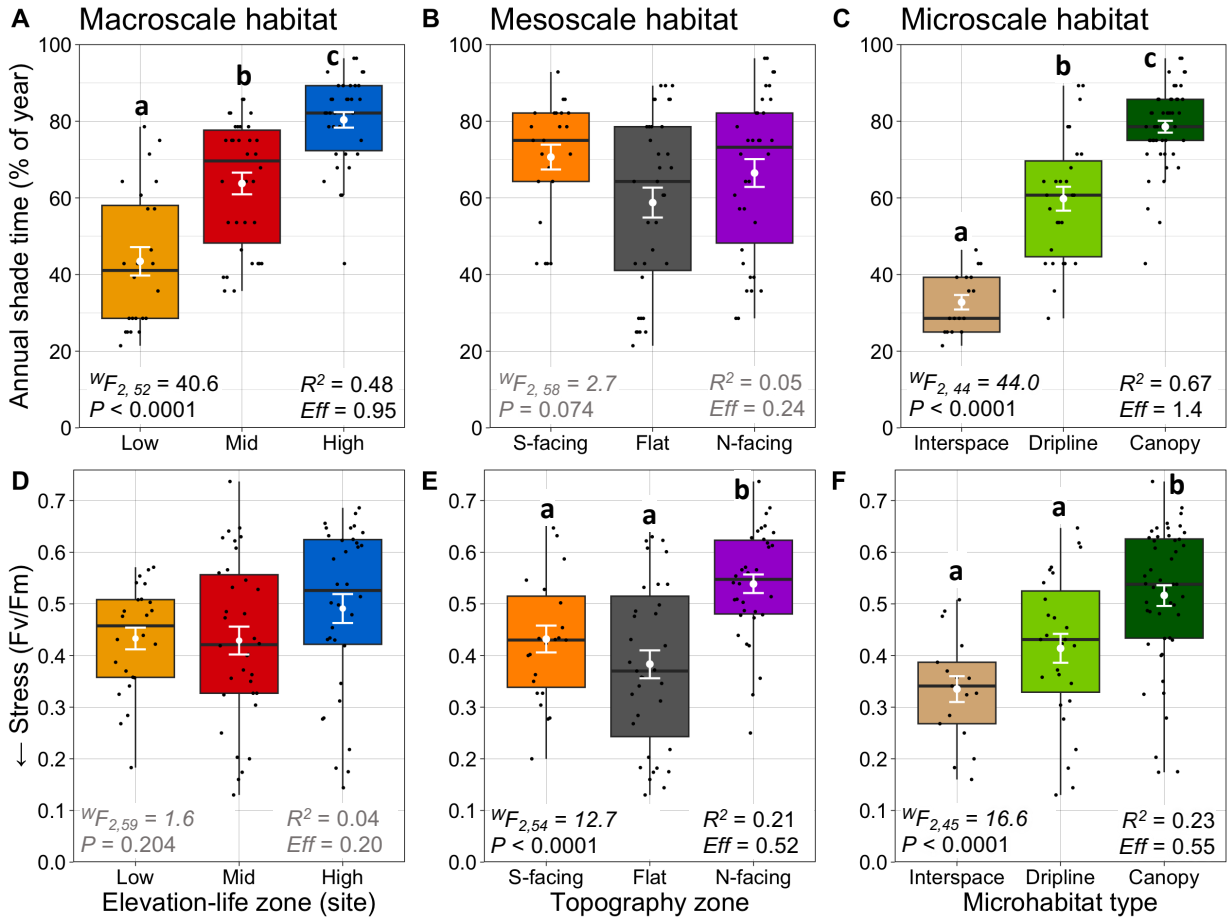

Figure 4. Boxplots of shade time (top row) and summer stress (bottom row) measured in 92 *Syntrichia caninervis* microhabitats pooled by scale of habitat structure: life zone (**A & D**), topography zone (**B & E**), and microhabitat type (**C & F**). Overlays include raw data (black points) and respective means (white points) with SE bars. Welch's ANOVA results, R^2, and Cohen's *F* (*Eff*) are shown for each panel. Letters indicate familywise Games-Howell significant differences between groups ($P < 0.05$) in post-hoc testing. Denominator degrees of freedom in F-statistics do not reflect sample size due to Welch's heterogeneity correction.

Figure 5. Patch appearance & shoot mortality: healthy & stressed *S. caninervis* in three Mojave Desert life zones

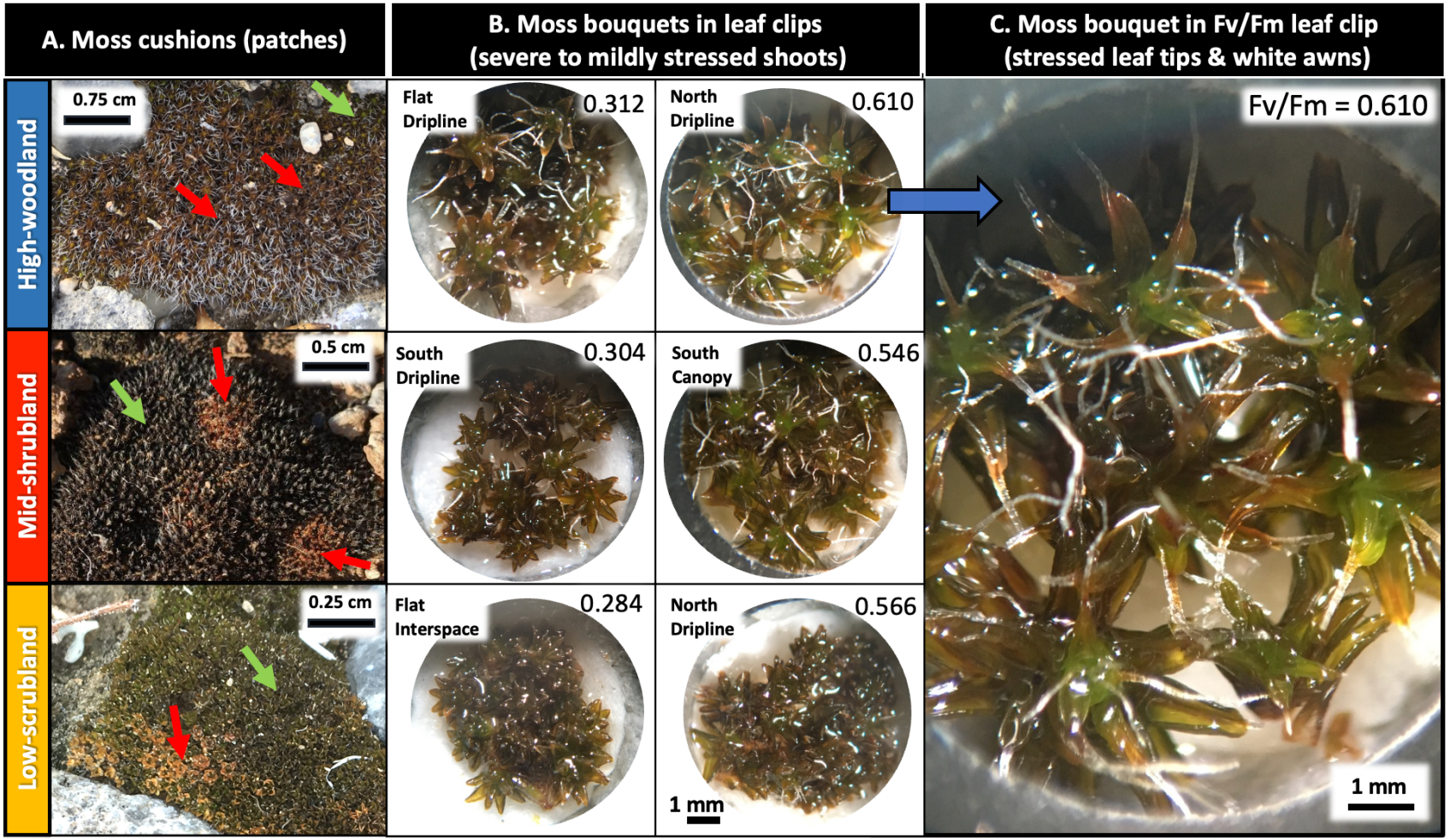

Figure 5. *Syntrichia caninervis* cushions by life zone site (***rows***) before sampling (**A**), in leaf clips during Fv/Fm assay (**B, C**). Healthy and mildly stressed shoots (***green arrows***) when wet (***A, Low & High sites***), often appeared green (**A**) or blackish-red from protective pigments (***A, Low site***). Severe stress can appear orange-green (***A, High site***). Dead (chlorotic) shoots appear orange (***A, red arrows***). **B.** Mild**,** moderate, and severely stressed shoots from a variety of microhabitats by site (*see also* ***Fig. 6***). **C.** Orange leaf tips evidence stressed shoots from the highest elevation life zone, a pinyon-juniper woodland with extensive shade cover.

Figure 6. *Syntrichia* summer stress distribution by life zone site

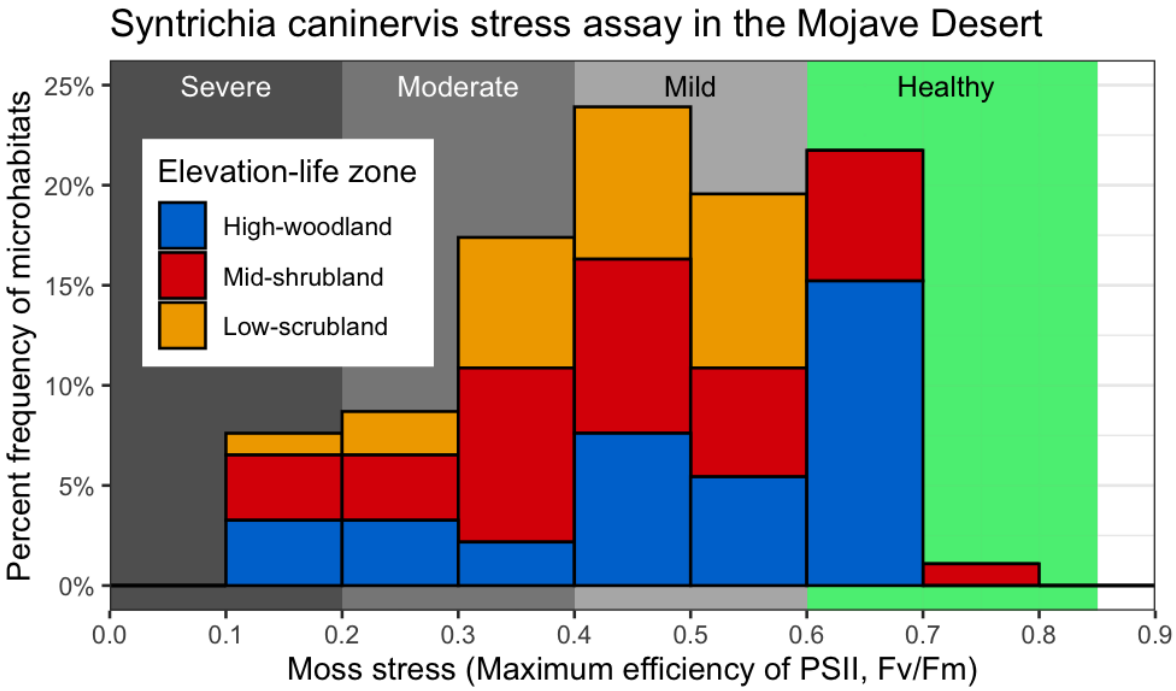

Figure 6. Frequency histogram of biocrust moss (*Syntrichia caninervis*) microhabitats with severe, moderate, and mild levels of photosynthetic stress (measured by the chlorophyll fluorescence metric, **Fv/Fm**) in 92 microsites colored by elevation-life zone site (see **Fig. 1**). Each bin is open on its maximum value (i.e. the bin [0, 0.1) does not include 0.1). Four colored bands indicate moss stress categories to aid climate vulnerability assessment in the Mojave Desert. Healthy mosses vary in their maximum Fv/Fm, so we have broadened "healthy" to begin at 0.6 (*see text*).

(of the lower 25th percentile; **Fig. 6**) were sourced from Flat-zones at all three life zones. These outliers included two interspace, three dripline, and one canopy microhabitat and had moderate annual shading ranging from 43 – 68%, except for one interspace microsite at the Low-scrubland that was shaded only 28% of the year. Extreme stress in these mosses was evident in chlorotic leaf tips (**Fig. 5b-c**). Exploring the shade timing of solar windows in these outliers will be done in a forthcoming paper (but see Clark 2020), but we suspect the lack of shade during midday may be a driving factor in extreme stress.

Moss stress vs three scales of habitat structure & buffering (Objective 4)

Habitat type ANOVAs – Contradicting our expectations, *S. caninervis* summer stress (Fv/Fm) did not differ on average by life zone ($^{Welch}F_{2,59}$ = 1.6, P = 0.204, **Fig. 4d**). Pooling topographical zones across sites, topography zone explained 21% of variation in stress with the N-facing zone supporting healthier mosses, on average, than the S-facing or flat zones, partly supporting our hypothesis ($^{Welch}F_{2,54}$ = 12.7, P < 0.0001, **Fig. 4e**). Microhabitat type explained 23% of variation in stress with healthier mosses under shrub canopies than in drip lines or interspaces, partly supporting our hypothesis ($^{Welch}F_{2,45}$ = 16.6, P < 0.0001, **Fig. 4f**).

Habitat buffering model – The full regression model including all multiscale buffering variables (elevation, PDIR, shade, and their interactions) was statistically significant explaining 55.4% of variance in moss stress ($F_{7,84}$ = 14.9, P < 0.0001; note this model should only be used for predictive purposes due to multicollinearity; **S2**). The highly significant reduced model (without site elevation) had acceptably stable beta estimates for PDIR, shade, and their interaction providing a model that can be reliably used for mechanistic inference ($F_{3,88}$ = 23.5, P < 0.0001, R^2 = 0.444, **Fig. 7**). Specifically, shade and PDIR were positively related to Fv/Fm (**Fig. 7b**); however, the full model indicated this relationship increased by life zone elevation (i.e., slopes became more positive with life zone elevation; **Fig. 7a**).

Life zone models (topography zone and shade) – Stress was not related to shade at the Low-scrubland, but the two topography zones explained 57% of variation in which mean Fv/Fm was higher on the N-facing zone than on the Flat zone ($^{Wald}F_{1,22}$ = 26.9, P < 0.0001, **Fig. 8c**). At the Mid-shrubland, shade and topography and their interaction explained 67% of variation in stress in which the Flat zone appears more positively related to shade than the N- and S-facing zones (*slopes not tested*; $^{Wald}F_{5,28}$ = 12.5, P < 0.0001, **Fig. 8b**). At the High-woodland, only shade was positively related to stress and explained 52% of variation ($^{Wald}F_{1,32}$ = 57.6, P < 0.0001; **Fig. 8a**).

DISCUSSION

This natural experiment allowed us to explore relationships between multiple scales of habitat structure, macroclimate buffering, and the *in-situ* summer stress response of a broadly distributed, keystone biocrust moss, *Syntrichia caninervis*. Our ecophysiological measurements tested the importance of environmental variation operating at landscape, topographic, and microhabitat scales in one of the harshest environments for which this species occurs globally, the Mojave Desert. We discuss how our results reveal signatures of ecophysiological resistance (***Part I***), signs of climate vulnerability (***Part II***), and inform next steps in a comprehensive vulnerability assessment for biocrust mosses like *S. caninervis* (***Part III***).

Figure 7. Summer stress vs habitat buffering proxies (elevation, PDIR, shade)

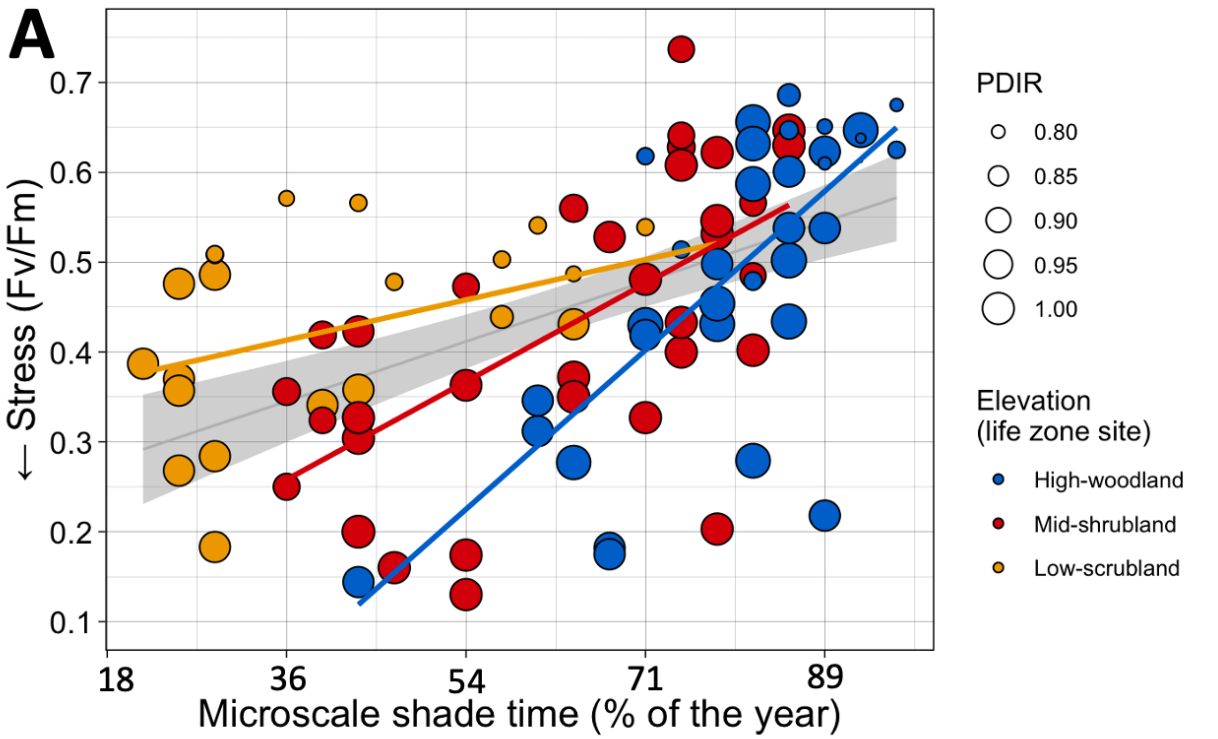

B

			Est.	2.5%	97.5%	t val.	p
F(3,88)	23.4537	(Intercept)	0.4542	0.4306	0.4778	38.2858	0.0000
R^2	0.4443	PDIR	-0.8147	-1.1289	-0.5004	-5.1516	0.0000
Adj. R^2	0.4254	Shade.Index	0.0132	0.0092	0.0173	6.5216	0.0000
Observations	92	PDIR:Shade.Index	0.0578	0.0053	0.1104	2.1869	0.0314
Dependent Y: Stress		Standard errors: OLS; Continuous predictors are mean-centered.					

Figure 7. A. Relationship of summer moss stress (lower Fv/Fm values indicate higher stress) of 92 *Syntrichia caninervis* microsites to habitat buffering proxies measured at three spatial scales: macroclimate (**elevation-life zone site: *point colors***), mesoscale potential direct incident radiation (***PDIR: circle size***), microscale shade time (***Shade.Index* in *B***), and their interaction (**:**). The OLS regression line for shade vs Stress is plotted with a 95% confidence interval in grey, and the interaction of elevation with shade is illustrated by varying slopes (*not tested*) of three OLS best fit lines plotted for each elevation-life zone. Elevation is shown graphically, but could not be included in the final model due to its multicollinearity with shade (see full model in **S2**). **B.** OLS regression results; residual plots are in **S3**.

Figure 8. Summer stress vs topography and shade by life zone

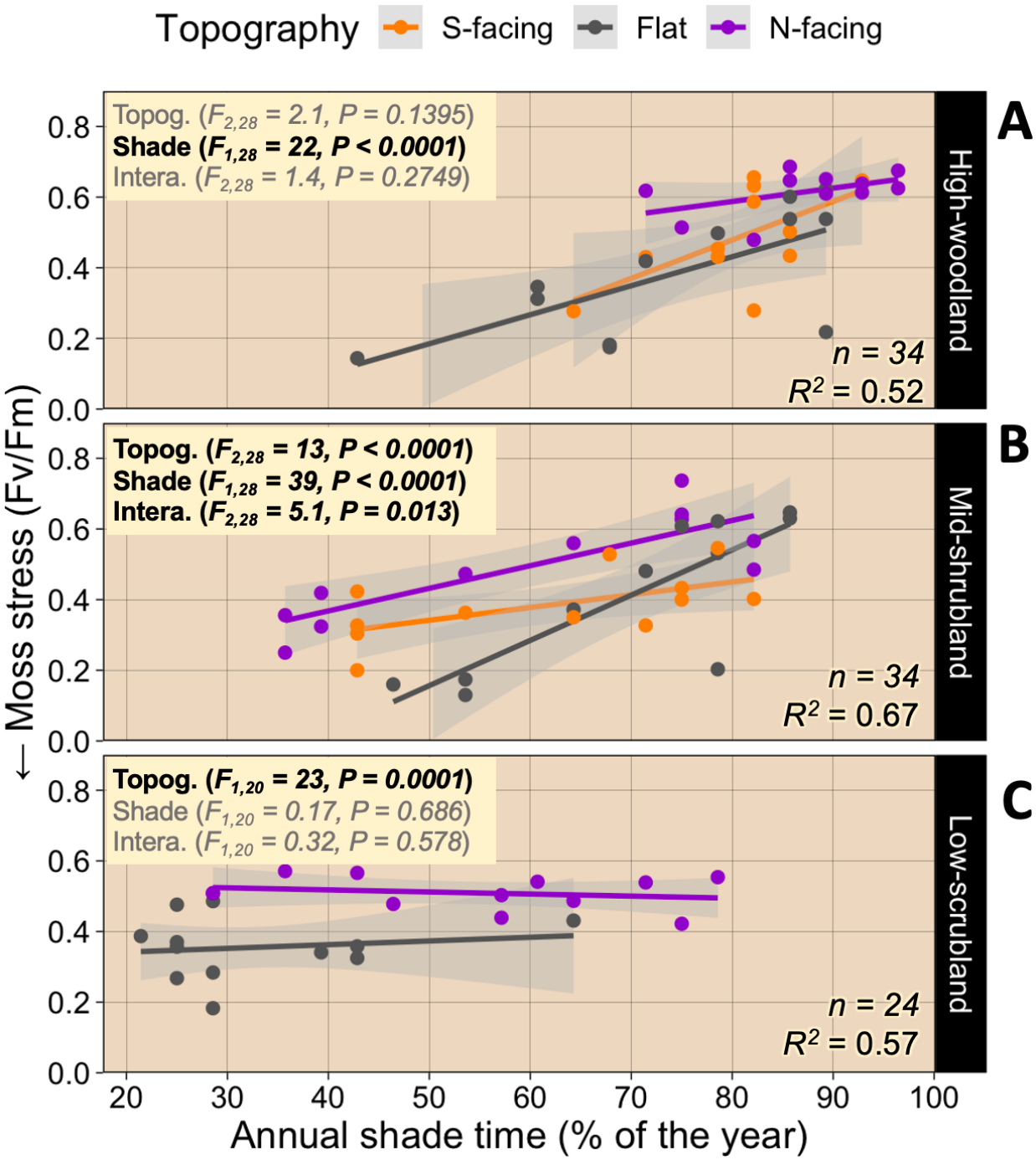

Figure 8. Three elevation-life zone site models and plots illustrate the linear relationship of summer moss stress of *Syntrichia caninervis* to topography (***Topog.***), annual shade time (***Shade***), and their interaction (***Intera.***). HCCM-ANCOVA results for each site (***panels***) include alpha significance for each term in the full model (**bold *P < 0.05***), R^2 for the reduced model (including only significant terms), and best fit lines with 95% C.I. (***grey bands***) from OLS regression. ***Note***: no mosses occurred on the S-facing slope of the Low-scrubland (see **Fig. 1c**).

Part I: Signatures of Resistance to Mojave Climate Stress

No moss mortality despite record-breaking summer climate – Despite an extreme summer in the Mojave Desert (2017), including record-breaking temperatures, low relative humidity, many small rain events, and over 45 days without rain, we report no patch mortality in the 94 *S. caninervis* microsites (i.e. all Fv/Fm > 0, **Fig. 6**). Temperatures reached record-breaking daily highs, and mean summer temperature was only 0.4°C from the hottest Nevada summer since 1985 (NOAA, 202). Drought periods fell within the highly variable but normal range for the Eastern Mojave (NOAA, 2020). When desiccated, extreme heat and extended drought are the least of Mojave climate stressors to which dryland mosses are sensitive (Stark 2017). In its commonly desiccated state, *S. caninervis* can tolerate intense solar loading, as Mojave genotypes can withstand 120°C (248°F) for 30 min – two times greater than typical Mojave summer air temperatures (Stark 2005, Stark et al. 2009). Notably, mosses are much more sensitive when hydrated and metabolically active – wet leaves of this species can die from exposure to 45°C (113°F) for >60 min (Stark & McLetchie 2006), a phenomenon which may have created the "sunspots" we observed as small circles of chlorotic shoots in some of our moss patches (**Fig. 5a**). Moreover, hydrated photosynthetic thermotolerance in *S. caninervis* is expected to increase alongside acclimation to rising $C0_2$ levels with climate change (Coe et al. 2012a).

Although increased variability in precipitation and drought is predicted for the Mojave Desert, the capacity for long-term desiccation tolerance of this and other dryland moss species should be resilient to increasingly erratic and record-breaking drought periods, which are already happening the American southwest (Zhang et al. 2021). Many dryland moss species can survive multiple years of dark, dry storage in herbaria (Stark et al. 2016), and the UV exposure while dry is offset in *S. caninervis* by protective leaf curling and pigmentation (Wu et al. 2013, Zhang et al. 2017), and prolonged UV exposure can increase desiccation tolerance in this species (Ekwealor et al. 2021).

Rate of drying is one of the most important stressors of desiccation – faster rates are more stressful than slower ones (e.g., Cruz de Carvalho et al. 2016, Greenwood et al. 2019). The recent lab study by Coe et al. (2021) demonstrated that extremely rapid drying (<10 min to leaf curling) and extreme intensity of desiccation (<1% RH) becomes lethal in *S. caninervis*. Natural rates of drying are controlled largely by event size, microhabitat humidity, and available substrate moisture (Stark 2017). Therefore, it follows that the absence of patch mortality in our study suggests that these experimentally extreme desiccation conditions have not occurred in situ for Mojave *S. caninervis* in recent years – patch mortality arising during or several years prior to this study would have been captured in our sample because dead moss persists for several years in drylands (Barker 2005). Nonetheless, warming and increased frequency of short, summer rain events may present lethal hydroperiods in the near future (Coe & Sparks 2014).

Protective roles of multiscale biocrust habitat – In the Mojave Desert and other drylands, habitat buffers like N-facing slopes and shade vegetation have been shown to reduce extremes in soil temperature, soil moisture, and moss thermal loading (Breshears et al. 1998, Bowker et al. 2000, Thompson et al. 2005, Kidron 2009), but our study is the first to report

physiologically significant multiscale habitat buffering in situ for a dryland moss. We found meso- and micro-scale habitat structure and buffering – created by topography and vegetation shading at three Mojave Desert life zones – was linked to increased summer stress resistance (i.e. lower Fv/Fm) in *S. caninervis*. In the remainder of **Discussion Part I**, we discuss the nature of these complex, multiscaled habitat relationships with moss photosynthetic stress physiology and highlight plausible mechanisms at play.

Microhabitat structure linked to diverse shrub shade buffering & moss stress resistance – Supporting our microscale shade hypothesis, our habitat survey determined high-shade "canopy microhabitats" to be the most common (**Appendix S1; see Supplemental Data with this article**) and support the healthiest *S. caninervis* patches across life zones wherein most mosses were shaded over 60% of the year (**Fig. 4c**, **Fig. 4f**). Furthermore, our novel shade buffering proxy, percent annual shade time (**Fig. 2**), appears most important to summer stress resistance at the Mid-shrubland and High-woodland, where shade was positively related to Fv/Fm within each mesoscale topography zone (**Fig. 8a-b**). Taken together, this evidence for shade buffering suggests that most shrub microhabitats in the Mojave Desert can provide an impressively high and physiologically meaningful shade buffer for *S. caninervis* (***see also Part II***).

The diversity of shade shrub species is another signature of resiliency we report for *S. caninervis* whose buffered dripline and canopy microhabitats were not restricted to a particular shrub species by life zone. Across the three life zones, over thirty plant species were present in the Sun Seeker solar windows (**Fig. 2**) contributing to the shade buffer either as immediate shade shrubs composing the microhabitat or via long-distance shade provisioning. At the Low-scrubland and Mid-shrubland, the dominant moss canopy shrubs were white bursage (*Ambrosia dumosa*) and blackbrush (*Coleogyne ramosissima*), respectively. Shade shrubs were most diverse at the High-woodland where sagebrush (*Artemisia* spp.), *Ceanothus greggii*, and *Ephedra viridis* were the most common moss canopy shrubs. Overall, we observed a niche preference for moss establishment under shorter shrubs with low-lying canopies (<0.5 m) as opposed to those with canopies >1 m high. Such shade shrub community structure is a clear aspect of summer stress resistance and will be analyzed in a future publication.

Few other studies have linked natural microhabitat variation to dryland moss photosynthetic stress. Alpert (1988) found a more positive carbon balance (another stress metric) in N- vs. S-facing rock mosses in semi-arid California, which was linked to increased microsite shading. Considering altered environments in the temperate Gurbantunggut Desert of China, Yin et al. (2017) measured healthier *S. caninervis* patches (e.g. greater Fv/Fm and antioxidant concentrations) under native shrub canopies compared to exposed patches in shrub-removal treatments. Stress metrics are important for species vulnerability assessments as they provide a warning signal for potential future lethality if climate conditions persist or worsen.

Multiscale habitat structure & buffering linked to stress resistance – We found strong support for our multiscale habitat buffering hypothesis elucidating important relationships and interactions between multiple scales of habitat structure and/or buffering with moss stress. Our life zone (**Fig. 8**) and habitat buffering (**Fig. 7**) models show that moderate to large (21 - 67%) variation in biocrust moss stress can be predicted by mesotopographical exposure (topography zone and PDIR), microhabitat shade, and their interactions.

Our buffering models suggest that two mesoscale (i.e., within-site) habitat buffers, PDIR and shade time, appear very important to moss summer resistance (**Fig. 7**) as do macroscale interactions with these finer-scale habitat features; **S2**). Working around the modeling restrictions of multicollinearity (between life zone elevation and shade; **Fig. 4a**) we graphically assessed the interaction of life zone with shade and found no evidence for a shade-stress relationship at the Low-scrubland; rather, we found strong evidence for topographical buffering upon further exploration in the life zone model, which also confirmed shade is not important on either topography zone (N-facing or Flat) in the Low-scrubland (**Fig. 8c**). The lack of a shade signal in this most arid and exposed life zone contradicted our expectation, however, we suggest topography buffering is superseding shade buffering on the steep N-facing zone, and that hydrological buffering by the drainage basin is superseding shade buffering on the Flat zone (i.e., where additional soil saturation may increase moss recovery time independent of the shade environment; **Fig. 1c**).

Our life zone models are the first to showcase evidence for two of our hypotheses: habitats with higher shade and/or N-facing slopes will support healthier mosses at the end of a Mojave summer (**Fig. 8**). site-level topography shapes unique buffering patterns for biocrust mosses that involve aspect, hydrological position, and shade (which is driven in part by life zone) and occasional interactions while providing evidence for

Small topographical exposure differences linked to biocrust moss stress – Constrained by erosion, biocrust moss establishment is often limited to gentler slopes, therefore, we were not surprised at the narrow range in topographical exposure across our topography zones (29% deviance; **Table 1b**) despite stabilizing desert pavement (TAC, *personal observation*) and our sampling design, which maximized the gradient in topography zone exposure at each site (**Fig. 1c**). Our results suggest that small differences in topographical exposure (6-14% deviance in PDIR) can be important to moss summer stress. For example, topography buffering appeared most important to stress (R^2= 0.60) at the Low-scrubland where the N-facing topography zone reduced exposure only 14% relative to the Flat zone (**Fig. 1c**, **Fig. 8c**). An an even smaller 7% topography buffer predicted 67% of moss stress when also considering shade and their interaction at the Mid-shrubland (**Fig. 8b**). Similarly, an 8% PDIR buffer (relative to the Flat-zone) is associated with the absence of moss on our reference S-facing slope at the Low-scrubland, suggesting a niche limitation for *S. caninervis* on soil surfaces receiving >1000 kJ/cm^2/yr in the creosote life zone of the Mojave Desert (**Table 1c**, **Fig. 1c**). We surveyed multiple S-facing slopes and could find no moss in this life zone.

However, our High-woodland model illustrates how topography buffering and shade can be confounded. The 22% topography buffer between opposing slopes of the ridge (**Table 1b**) was correlated with shade because the steep, N-facing topography zone was also the most shaded of the three topography zones at this site (**Fig. 8a**). Such ecological confoundedness is often unavoidable – greater shade on northerly-facing slopes is created in part by topographical shading (i.e., created by the northerly facing slope itself) and by higher vegetation density (Pelletier et al. 2017). Untangling these complex multiscale relationships would require advanced modeling techniques with larger sample sizes and warrants further study. However, we suggest that disentangling correlated fine-scale habitat features is less important for climate change vulnerability. Rather, we suggest parsing the relative contribution of fine-scale (within-site) vs. macroscale (across-sites or life zones) habitat structure to stress variation, and

illustrating covariance between predictors, which we have done here in the High-woodland interaction plot (**Figure 8a**).

Part II: Signs of Vulnerability to Climate Change

High elevation refugia may not shelter biocrust mosses as predicted – Bryophyte community responses to climate change may not mirror those of tracheophytes, many of which are predicted to migrate to higher elevations as aridity increases (Gignac 2001, Slack 2011). *S. caninervis* has a broad geographic and ecological amplitude (BFNA 2007, eFloras 2023*,* María Ros et al. 1999) compared to many tracheophytes whose distributions are usually constrained to narrower elevational bands and single continents (Patiño & Vanderpoorten 2018). We had anticipated that the cooler, wetter climate and mountain topography at the High-woodland (2065 m, **Table 1a**) would reduce summer moss stress relative to the Low-scrubland, but found no such pattern (**Fig. 4a**, **Fig. 6**). The lack of signal for high-elevation refugia given this 1200-m macroclimate buffer is surprising, and in response, we are testing (with environmental sensors) whether microclimate variation in summer is greater across microhabitats than across life zones. The broad ecological amplitude of many mosses is a function of their ability to exploit similarly buffered microhabitats that exist across vastly different ecosystems (Ladrón de Guevara & Maestre). This may indeed be the case for *S. caninervis* as we documented the species living beneath the shade canopies of over fifteen different shrub or tree species in DNWR. Therefore we report signals that "shrub microhabitat refugia", rather than high-elevation macroscale refugia may best protect biocrust moss in future climates assuming the shrubs themselves are resistant to climate stress.

Moss dependency on shrubs may increase future vulnerability – *S. caninervis* microhabitats under shrubs were 63% healthier (higher Fv/Fm) than interspaces (**Fig. 6e**) building evidence for physiologically significant habitat buffering. Most moss patches were located within 0.5 m of a shrub's dripline and, in most cases, we observed the largest patches on soil beneath shrub canopies. This apparent shrub dependency may increase future vulnerability of biocrust mosses in the Mojave Desert if dominant shrub species experience die-back or range shifts with climate change (e.g., Ladrón de Guevara & Maestre 2022). A shrub removal experiment by Yin et al. (2017) on in situ *S. caninervis* found increased stress (reduced Fv/Fm) and shorter spring hydroperiods for treated than untreated mosses, raising concern for rapid physiological responses with unknown long-term effects (beyond 9 mo). In nature, effects of any climate-induced shrub die-back will be slower with a longer lag time because significant shade reduction from a dying shrub will not incur until after the canopy fully degrades, which could be multiple years in the Mojave Desert where wood decay is slow. Nonetheless, although our study explicitly avoided sampling mosses under damaged shrub canopies, we suggest future research incorporate ecological facilitation by nurse shrubs into local biocrust vulnerability assessments.

Results may underestimate population stress & vulnerability – Given the extreme aridity of summer 2017 in DNWR (**Table 1**), perhaps it is not surprising that 33% of the *S. caninervis* microsites showed signs of moderate and severe climate stress (**Fig. 6**). Such reduced PSII efficiency (low Fv/Fm) in mosses is often called photoinhibition, a state of compromised efficiency in photosynthesis light reactions resulting from damaged or deactivated PSII reaction centers and/or acclimatory changes in nonphotochemical quenching (Demmig-Adams & Adams

2006). In desiccation tolerant mosses, photoinhibition may be caused by many factors including rapid drying, low water potential, reactive oxygen species, high temperatures, excess light, and UV damage (Takács et al. 1999, Proctor 2001, Proctor et al. 2007b, Ekwealor et al. 2021). Severe photoinhibition (Fv/Fm < 0.2) can precede mortality in plant tissues (e.g. Coe et al. 2020), however, some mosses do recover from such low levels of Fv/Fm (e.g., Cruz de Carvalho 2001, Ekwealor et al. 2021). We measured significant Fv/Fm recovery in our 94 moss samples within 24 hrs in vivo; these resiliency results will be presented in a forthcoming publication (see Clark 2020). Given this apparent resiliency in vivo, we urge further research to determine in what climate scenarios photoinhibition becomes damaging to long-term productivity and survival in bryophytes (e.g. Hájek & Vicherová 2013) by monitoring moss stress and mortality over multiple years and acute climate events.

The climate vulnerability signal we present for the three life zone populations of *S. caninervis* (**Fig. 6**) should represent most microhabitats in the Mojave Desert. However, our design targeted the largest, high-density moss microsites along the three habitat-exposure gradients excluding those with low-density moss and/or damaged shrub canopies (from die-back or broken branches; *see* ***Methods***). Concordantly, we excluded the least favorable microsites – in most cases high-exposure interspaces – often dominated by lichens, and thus, our findings may underestimate the most stressed moss patches in the Mojave.

High variability in summer stress may foreshadow ecological transition – Variability in ecosystems has been shown to predict ecological regime shifts (Carpenter & Brock 2006). The high summer stress variability we observed in three life zone populations of *S. caninervis* may be a strong indicator of declining resilience in this species and may foreshadow a biocrust community type transition. For example, several climate manipulation experiments predict that lichen-dominated biocrust with few mosses may quickly transition to lichen-cyanobacterial biocrust under future climates (He et al. 2016, Li et al. 2018). Such reductions in the frequency and/or abundance of *S. caninervis* throughout its current range could alter biocrust function, as the strength of ecological services facilitated by biocrust mosses is largely a function of their biomass. Many studies predict that climate change will reduce moss biomass and thus their functional roles in future drylands causing ecosystem-wide consequences at local and regional scales while potentially accelerating desertification (e.g., Coe & Sparks 2014, Rodriguez-Caballero et al. 2018, Ladrón de Guevara and Maestre 2022).

CONCLUSIONS

Part III: Can biocrust mosses hide from climate change?

Patterns in our natural experiment corroborate the warning of previous reviews that climate change responses of bryophytes may be more complex than most plants given their unique poikilohydric physiologies and fine-scale habitats, which require different temporal (i.e. hydroperiod) and spatial (i.e. microhabitat) scales of study than for large, homiohydric tracheophytes (e.g., He et al. 2016, Ladrón de Guevara & Maestre 2022). We recommend seasonal and multiyear monitoring with a multiscale habitat framework to strengthen climate change vulnerability assessments for keystone species (Clark 2020). Elucidating the presence of potential micro- or macrorefugia should be a primary goal (Ashcroft 2010). For many dryland species who lack long-distance dispersal (Zanatta et al. 2020), microrefugia should be more important – because such species may be unable to track the rate of rapid climate change.

Identifying and protecting key microrefugia may mitigate the need for assisted migration or conservation efforts. For biocrust mosses, their delicate communities also require efficient, minimally invasive monitoring while there is still time for management planning and conservation action.

As a model framework, we have delineated habitat distribution and complexity for a keystone biocrust moss, *Syntrichia caninervis*, in the Mojave Desert. We have used spatially nested (i.e., efficient) chlorophyll fluorescence measurements (i.e., minimally invasive shoot sampling) to link multiscale habitat structure with climate buffering and with moss summer-stress resistance. Our findings present evidence for the presence of abiotically and biotically variable microrefugia – rather than high-elevation macrorefugia – within each life zone of a Mojave Desert aridity gradient. Such microrefugia should be critical for the persistence of this species in drylands, as this moss rarely produces spores (Smith & Stark 2014, Benassi et al. 2011), the bryophyte propagules most adapted to long-distance dispersal via wind (Carter 2021), which may slow migration rates.

With its broad ecological range and strong desiccation tolerance, we need monitoring of *S. caninervis* in other deserts where it is also important in biocrust, but where its resilience is unknown (e.g. Great Basin Desert, Africa's Sahel, China's Gurbantunggut Plateau). Advancing the vulnerability assessment of this species within this climatically extreme part of its global distribution, we conclude *S. caninervis* appears capable of "hiding" in buffered microhabitats during an extreme Mojave summer. Contrary to most climate change experiments predicting low moss resiliency to increasing aridity and altered precipitation patterns in drylands, our findings present the possibility that at least one ecologically critical biocrust moss may be more prepared for a changing Mojave climate than previously thought, as long as associated shrub mortality does not accelerate.

Acknowledgments

We thank the doctoral committee of TAC (Drs. Daniel Thompson, Sandra Catlins, Dale Devitt, and Peter Nelson) for assistance in the development of this University of Nevada Las Vegas (UNLV) dissertation project. We thank Amy Sprunger for logistical support in field research at the Desert National Wildlife Refuge. We thank Brian Bird for infrastructural support working within the NevCAN Network. Field sampling, lab work, and data management were aided by many volunteers to which we are grateful. The research was supported by fellowships and grants to TAC including the UNLV Summer Doctoral Research Fellowship and the UNLV President's Foundation Graduate Research Fellowship, the American Bryological and Lichenological Society Anderson and Crum Field Research Award, and the UNLV Graduate and Professional Student Association Summer Research Scholarship.

Author Contributions

TAC conceptualized this dissertation research with advisership of LRS and DD. TAC performed all analyses, made graphics, and wrote the original draft. TAC and AR performed field investigations. TAC, AR, and JG performed the laboratory investigation. All authors contributed to manuscript review and editing.

Data Availability

Data and R code used in this manuscript are openly available on GitHub at https://github.com/TreesaClark/Syntrichia_summer_stress.

Supporting Information

Additional supporting information may be found online in the Supporting Information section at the end of the article.

S1. Microhabitat type relative frequency by life zone site.

S2. Correlation and regression table for the full habitat buffering model.

S3. Residual diagnostic plots for the reduced habitat buffering regression model.

Literature Cited

Abed, R. M. M., A. Tamm, C. Hassenrück, A. N. Al-Rawahi, E. Rodríguez-Caballero, S. Fiedler, S. Maier, and B. Weber. 2019. Habitat-dependent composition of bacterial and fungal communities in biological soil crusts from Oman. *Scientific Reports* 9: 1–16.

Ackerman, T. L. 2003. A flora of the Desert National Wildlife Range, Nevada. *Mentzelia: The Journal of the Nevada Native Plant Society* 7.

Alpert, P. 1985. Distribution Quantified by Microtopography in an Assemblage of Saxicolous Mosses. *Vegetatio* 64: 131–139.

Alpert, P. 1988. Survival of a desiccant-tolerant moss, Grimmia laevigata, beyond its observed microdistributional limit. *Journal of Bryology* 15: 219–227.

Amrhein, V., S. Greenland, and B. McShane. 2019. Retire Statistical Significance. *Nature* 567: 305–307.

Ashcroft, M. B. 2010. Identifying refugia from climate change. *Journal of Biogeography* 37: 1407–1413.

Baker, N. R. 2008. Chlorophyll Fluorescence: A Probe of Photosynthesis In Vivo. *Annual Reviews in Plant Biology* 59: 89–113.

Barker, D. H., L. R. Stark, J. F. Zimpfer, N. D. McLetchie, and S. D. Smith. 2005. Evidence of drought-induced stress on biotic crust moss in the Mojave Desert. *Plant, Cell and Environment* 28: 939–947.

Belnap, J., S. L. Phillips, and M. E. Miller. 2004. Pulse events and arid ecosystems: Response of desert biological soil crusts to alterations in precipitation frequency. *Oecologia* 141: 306–316.

Belnap, J. 2003. The World at Your Feet- Desert Biological Soil Crusts. *Frontiers in Ecology and the Environment* 1: 181–189.

BFNA Editorial Committee ed. . 2007. Bryophyte Flora of North America: Bryophytes North of Mexico. Volumes 27. Oxford University Press, New York.

Bowker, M. A., L. R. Stark, D. N. Mcletchie, and B. D. Mishler. 2000. Sex Expression, Skewed Sex Ratios, and Microhabitat Distribution in the Dioecious Desert Moss Syntrichia caninervis (Pottiaceae). *American Journal of Botany* 87: 517–526.

Bowker, M. A., J. Belnap, B. Büdel, C. Sannier, N. Pietrasiak, D. J. Eldridge, and V. Rivera-Aguilar. 2016. Controls on Distribution Patterns of Biological Soil Crusts at Micro- to Global Scales. *In* B. Weber, B. Büdel, and J. Belnap [eds.], Biological Soil Crusts: An Organizing Principle in Drylands, 173–197. Springer International Publishing, Switzerland.

Bowker, M. A., F. T. Maestre, and R. L. Mau. 2013. Diversity and Patch-Size Distributions of Biological Soil Crusts Regulate Dryland Ecosystem Multifunctionality. *Ecosystems* 16: 923–933.

Breshears, D. D., J. W. Nyhan, C. E. Heil, and B. P. Wilcox. 1998. Effects of woody plants on microclimate in a semiarid woodland: Soil temperature and evaporation in canopy and intercanopy patches. *International Journal of Plant Sciences* 159: 1010–1017.

Brinda, J. C., C. Fernando, and L. R. Stark. 2011. Ecology of Bryophytes in Mojave Desert Biological Soil Crusts: Effects of Elevated CO2 on Sex Expression, Stress Tolerance, and Productivity in the Moss Syntrichia caninervis Mitt. *In* Z. Tuba, N. G. Slack, and L. R. Stark [eds.], Bryophyte Ecology and Climate Change, 169–189. Cambridge University Press, Cambridge.

Brinda, J. C., J. A. Jauregui-lazo, M. J. Oliver, and B. D. Mishler. 2021. Notes on the genus *Syntrichia*

with a revised infrageneric classification and the recognition of a new genus Syntrichiadelphus (Bryophyta , Pottiaceae). *Phytologia* 103: 90–103.
Carpenter, S. R., and W. A. Brock. 2006. Rising variance: a leading indicator of ecological transition. *Ecology Letters* 9: 311–318.
Clark, T. A. 2020. Can desert mosses hide from climate change? The Ecophysiological Importance of Habitat Buffering & Water Relations to the Stress Response of a Keystone Biocrust Moss. University of Nevada Las Vegas.
Clark, T. A. 2012. Bryophyte Floristics and Ecology in Grand Canyon National Park.
Coe, K. K., J. Belnap, E. E. Grote, and J. P. Sparks. 2012. Physiological ecology of desert biocrust moss following 10 years exposure to elevated CO2: Evidence for enhanced photosynthetic thermotolerance. *Physiologia Plantarum* 144: 346–356.
Coe, K. K., J. Belnap, and J. P. Sparks. 2012. Precipitation-driven carbon balance controls survivorship of desert biocrust mosses. *Ecology* 93: 1626–1636.
Coe, K. K., J. L. Greenwood, M. L. Slate, Clark, T. A., J. C. Brinda, K. M. Fisher, B. D. Mishler, M. A. Bowker, et al. 2020. Strategies of Desiccation Tolerance vary across Life Phases in the Moss *Syntrichia caninervis*. *American Journal of Botany* 108.2: 249–262.
Coe, K. K., and J. P. Sparks. 2014. Physiology-based prognostic modeling of the influence of changes in precipitation on a keystone dryland plant species. *Oecologia* 176: 933–942.
Crawley, M. J. 2007. The R Book. 1st ed. John Wiley & Sons, Chichester, England.
Cruz De Carvalho, R., C. Branquinho, and J. M. da Silva. 2011. Physiological consequences of desiccation in the aquatic bryophyte Fontinalis antipyretica. *Planta* 234: 195–205.
Cruz de Carvalho, R., M. Catalá, C. Branquinho, J. Marques da Silva, and E. Barreno. 2016. Dehydration rate determines the degree of membrane damage and desiccation tolerance in bryophytes. *Physiologia Plantarum*.
Demmig-Adams, B., and W. W. Adams. 2006. Photoprotection in an ecological context: The remarkable complexity of thermal energy dissipation. *New Phytologist* 172: 11–21.
Douma, J. C., and J. T. Weedon. 2019. Analysing continuous proportions in ecology and evolution: A practical introduction to beta and Dirichlet regression. *Methods in Ecology and Evolution* 10: 1412–1430.
DRI. 2020. Desert Research Institute, Western Regional Climate Center. *Nevada EPSCOR Sheep Range Transect Stations*. Website http://wrcc.dri.edu/SRtransect/ [accessed 1 March 2020].
eFloras. 2023. eflora Moss Flora of China, Volume 2. Missouri Botanical Garden and Harvard University Herbaria, St. Louis, MO and Cambridge, MA.
Ekwealor, J. T. B., T. A. Clark, O. Dautermann, A. Russell, S. Ebrahimi, L. R. Stark, K. K. Niyogi, and B. D. Mishler. 2021. Natural ultraviolet radiation exposure alters photosynthetic biology and improves recovery from desiccation in a desert moss. *Journal of Experimental Botany* 72: 4161–4179.
Elbert, W., B. Weber, S. Burrows, J. Steinkamp, B. Büdel, M. O. Andreae, and U. Pöschl. 2012. Contribution of cryptogamic covers to the global cycles of carbon and nitrogen. *Nature Geoscience* 5: 459–462.
Ferrenberg, S., S. C. Reed, and J. Belnap. 2015. Climate change and physical disturbance cause similar community shifts in biological soil crusts. *Proceedings of the National Academy of Sciences* 112: 12116–12121.
Fisher, K., J. S. Jefferson, and P. Vaishampayan. 2020. Bacterial Communities of Mojave Desert

Biological Soil Crusts Are Shaped by Dominant Photoautotrophs and the Presence of Hypolithic Niches. *Frontiers in Ecology and Evolution* 7: 1–11.
Fligner, M. A., and T. J. Killeen. 1976. Distribution-free two sample tests for scale. *Journal of American Statistical Association* 71: 210–213.
Fox, J., and S. Weisberg. 2019. An R Companion to Applied Regression. 3rd ed. Sage, Thousand Oaks, CA.
Gignac, L. D. 2001. Bryophytes as Indicators of Climate Change. *The Bryologist* 104: 410–420.
Gotelli, N. J., and A. M. Ellison. 2013. A Primer of Ecological Statistics. 2nd ed. Sinauer Associates, Inc., Sunderland, MA, USA.
Greenwood, J. L., L. R. Stark, and L. P. Chiquoine. 2019. Effects of rate of drying, life history phase, and ecotype on the ability of the moss, Bryum argenteum, to survive desiccation events and the influence on conservation and selection of material for restoration. *Frontiers in Ecology and Evolution* 7: 388.
Guo, Y., and Y. Zhao. 2018. Effects of storage temperature on the physiological characteristics and vegetative propagation of desiccation-tolerant mosses. *Biogeosciences* 15: 797–808.
Hájek, T., and E. Vicherová. 2014. Desiccation tolerance of Sphagnum revisited: a puzzle resolved. *Plant Biology* 16: 765–773.
Hamerlynck, E. P., Z. Tuba, Z. Csintalan, Z. Nagy, G. Henebry, and D. Goodin. 2000. Diurnal variation in photochemical dynamics and surface reflectance of the desiccation-tolerant moss, Tortula ruralis. *Plant Ecology* 151: 55–63.
He, X., K. S. He, and J. Hyvönen. 2016. Will bryophytes survive in a warming world? *Perspectives in Plant Ecology, Evolution and Systematics* 19: 49–60.
Kassambara, A. 2023. rstatix: Pipe-Friendly Framework for Basic Statistical Tests. *R package version 0.7.2*. Website https://cran.r-project.org/package=rstatix.
Kidron, G. J. 2009. The effect of shrub canopy upon surface temperatures and evaporation in the Negev Desert. *Earth Surface Processes and Landforms* 34: 123–132.
Ladrón De Guevara, M. and F. T. Maestre. 2022. Ecology and responses to climate change of biocrust-forming mosses in drylands. Journal of Experimental Botany 73: 4380–4395.
Lafuente, A., M. Berdugo, M. Ladrón de Guevara, B. Gozalo, and F. T. Maestre. 2018. Simulated climate change affects how biocrusts modulate water gains and desiccation dynamics after rainfall events. *Ecohydrology* 11: 1–10.
Lakens, D. 2013. Calculating and reporting effect sizes to facilitate cumulative science: a practical primer for t-tests and ANOVAs. *Frontiers in Psychology* 4: 863.
Langsrud, Ø. 2003. ANOVA for unbalanced data: Use Type II instead of Type III sums of squares. *Statistics and Computing* 13: 163–167.
Li, X.-R., R.-L. Jia, Z.-S. Zhang, P. Zhang, and R. Hui. 2018. Hydrological response of biological soil crusts to global warming: A ten-year simulative study. *Global Change Biology* 24: 4960–4971.
Logan, M. 2010. Biostatistical Design and Analysis Using R. Wiley-Blackwell, Oxford, UK.
Long, J. S., and L. H. Ervin. 2000. Using Heteroscedasticity Consistent Standard Errors in the Linear Regression Model. *The American Statistician* 54: 217–224.
McCune, B., and D. Keon. 2002. Equations for potential annual direct incident radiation and heat load. *Journal of Vegetation Science* 13: 603–606.
McCune, B. 2007. Improved estimates of incident radiation and heat load using non-parametric regression against topographic variables. *Journal of Vegetation Science* 18: 751–754.

Mensing, S., S. Strachan, J. Arnone, L. Fenstermaker, F. Biondi, D. Devitt, B. Johnson, et al. 2013. A network for observing great basin climate change. *EOS Transactions American Geophysical Union* 94: 105–106.
Munzi, S., Z. Varela, and L. Paoli. 2019. Is the length of the drying period critical for photosynthesis reactivation in lichen and moss components of biological soil crusts? *Journal of Arid Environments* 166: 86–90.
Murchie, E. H., and T. Lawson. 2013. Chlorophyll fluorescence analysis: A guide to good practice and understanding some new applications. *Journal of Experimental Botany* 64: 3983–3998.
Nash, T. H., S. L. White, and J. E. Marsh. 1977. Lichen and Moss Distribution and Biomass in Hot Desert Ecosystems. *The Bryologist* 80: 470–479.
NCCP. 2018. Nevada Climate Change Portal. *The Nevada Climate-Ecohydrological Assessment Network (NevCAN)*. Website http://sensor.nevada.edu/NCCP/Default.aspx.
NOAA. 2017. Climate at a Glance: Divisional Rankings. *NOAA National Centers for Environmental Information*. Website https://www.ncdc.noaa.gov/cag/ [accessed 24 February 2020].
Papadatos, S., A. C. Charalambous, and V. Daskalakis. 2017. A pathway for protective quenching in antenna proteins of Photosystem II. *Scientific Reports* 7: 1–13.
Patiño, J., and A. Vanderpoorten. 2018. Bryophyte biogeography. *Critical Reviews in Plant Sciences* 0: 1–35.
Pelletier, J. D., G. A. Barron-Gafford, H. Gutiérrez-Jurado, E. L. S. Hinckley, E. Istanbulluoglu, L. A. McGuire, G. Y. Niu, et al. 2018. Which way do you lean? Using slope aspect variations to understand Critical Zone processes and feedbacks. Earth Surface Processes and Landforms 43: 1133–1154.
Pietrasiak, N., R. E. Drenovsky, L. S. Santiago, and R. C. Graham. 2014. Biogeomorphology of a Mojave Desert landscape - Configurations and feedbacks of abiotic and biotic land surfaces during landform evolution. *Geomorphology* 206: 23–36.
Proctor, M. C. F. 2009. Physiological Ecology. *In* B. Goffinet, and J. A. Shaw [eds.], Bryophyte Biology, 237–268. Cambridge University Press, Cambridge, United Kingdom and New York, New York.
Proctor, M. C. F., M. J. Oliver, A. J. Wood, L. R. Stark, N. L. Cleavitt, B. D. Mishler, P. Alpert, et al. 2007. Desiccation-tolerance in bryophytes: a review. *The Bryologist* 110: 595–621.
Proctor, M. C. F. 2001. Patterns of desiccation tolerance and recovery in bryophytes. *Plant growth regulation* 35: 147–156.
R-Core-Development-Team. 2023. R: A language and environment for statistical computing.
Reed, S. C., K. K. Coe, J. P. Sparks, D. C. Housman, T. J. Zelikova, and J. Belnap. 2012. Changes to dryland rainfall result in rapid moss mortality and altered soil fertility. *Nature Climate Change* 2: 752–755.
Ros, R. M., M. J. Cano, and J. Guerra. 1999. Bryophyte checklist of northern Africa. *Journal of Bryology* 21: 207--244.
Ruxton, G. D., and G. Beauchamp. 2008. Time for some a priori thinking about post hoc testing. *Behavioral Ecology* 19: 690–693.
Scheffers, B. R., D. P. Edwards, A. Diesmos, S. E. Williams, and T. a. Evans. 2014. Microhabitats reduce animal's exposure to climate extremes. *Global Change Biology* 20: 495–503.
Seager, R., M. Ting, I. Held, Y. Kushnir, J. Lu, G. Vecchi, H.-P. Huang, et al. 2007. Model projections of an imminent transition to a more arid climate in southwestern North America. *Science* 316:

1181–1184.
Seager, R., and G. A. Vecchi. 2010. Greenhouse warming and the 21st century hydroclimate of southwestern North America. *Proceedings of the National Academy of Sciences* 14: 21277–21282.
Seppelt, R., A. Downing, K. K. Coe, Y. Zhang, and J. Zhang. 2016. Bryophytes Within Biological Soil Crusts. *In* B. Weber, B. Büdel, and J. Belnap [eds.], Biological Soil Crusts: An Organizing Principle in Drylands, 101–120. Springer International Publishing, AG Switzerland.
Shi, H., Z. Wen, D. Paull, and M. Guo. 2016. A framework for quantifying the thermal buffering effect of microhabitats. *Biological Conservation* 204: 175–180.
Slack, N. G. 2012. The Ecological Value of Bryophytes as Indicators of Climate Change. *In* Z. Tuba, N. G. Slack, and L. R. Stark [eds.], Bryophyte Ecology and Climate Change, 3–12. Cambridge University Press, Cambridge.
Smith, R. J., and L. R. Stark. 2014. Habitat vs. dispersal constraints on bryophyte diversity in the Mojave Desert, USA. *Journal of Arid Environments* 102: 76–81.
Stark, L. R., and D. Nicholas McLetchie. 2006. Gender-specific heat-shock tolerance of hydrated leaves in the desert moss *Syntrichia caninervis*. *Physiologia Plantarum* 126: 187–195.
Stark, L. R. 2017. Ecology of desiccation tolerance in bryophytes: A conceptual framework and methodology. *The Bryologist* 120: 130–165.
Stark, L. R. 2005. Phenology of patch hydration, patch temperature and sexual reproductive output over a four-year period in the desert moss *Crossidium crassinerve*. *Journal of Bryology* 27: 231–240.
Stark, L. R., J. C. Brinda, and N. D. McLetchie. 2011. Effects of increased summer precipitation and N deposition on Mojave Desert populations of the biological crust moss Syntrichia caninervis. *Journal of Arid Environments* 75: 457–463.
Stark, L. R., J. L. Greenwood, and J. C. Brinda. 2016. Desiccated Syntrichia ruralis shoots regenerate after 20 years in the herbarium. *Journal of Bryology* 39: 85–93.
Stark, L. R., D. N. McLetchie, and S. P. Roberts. 2009. Gender differences and a new adult eukaryotic record for upper thermal tolerance in the desert moss Syntrichia caninervis. *Journal of Thermal Biology* 34: 131–137.
Stovall, M. S., A. C. Ganguli, J. W. Schallner, A. M. Faist, Q. Yu, and N. Pietrasiak. 2022. Can biological soil crusts be prominent landscape components in rangelands? A case study from New Mexico, USA. *Geoderma* 410: 115658.
Takács, Z., Z. Csintalan, L. Sass, E. Laitat, I. Vass, and Z. Tuba. 1999. UV-B tolerance of bryophyte species with different degrees of desiccation tolerance. *Journal of Photochemistry and Photobiology B: Biology* 48: 210–215.
Thompson, D. B., L. R. Walker, F. H. Landau, and L. R. Stark. 2005. The influence of elevation, shrub species, and biological soil crust on fertile islands in the Mojave Desert, USA. *Journal of Arid Environments* 61: 609–629.
Warton, D. I., and F. C. K. Hui. 2011. The arcsine is asinine: the analysis of proportions in ecology. *Ecology* 92: 3–10.
Welch, B. L. 1951. On the comparison of several mean values: an alternative approach. *Biometrika* 38: 330–336.
White, H. 1980. A Heteroskedastic-Consistent Covariance Matrix Estimator and a Direct Test of Heteroskedasticity. *Econometrica* 48: 817–838.

Wickham, H. 2016. ggplot2: Elegant Graphics for Data Analysis. Springer-Verlag, New York.
Wickham, H., M. Averick, J. Bryan, W. Chang, L. D. McGowan, R. François, G. Grolemund, et al. 2019. Welcome to the {tidyverse}. *Journal of Open Source Software* 4: 1686.
Williams, A. J., B. J. Buck, D. A. Soukup, and D. J. Merkler. 2013. Geomorphic controls on biological soil crust distribution: A conceptual model from the Mojave Desert (USA). *Geomorphology* 195: 99–109.
Williams, S. E., C. Moritz, L. P. Shoo, J. L. Isaac, A. a Hoffmann, G. Langham, C. Moritz, et al. 2008. Towards an Integrated Framework for Assessing the Vulnerability of Species to Climate Change. *PLoS biology* 6: e325.
Xiao, B., K. Hu, T. Ren, and B. Li. 2015. Moss-dominated biological soil crusts significantly influence soil moisture and temperature regimes in semiarid ecosystems. *Geoderma* 263: 35–46.
Yin, B. F., Y.-M. Zhang, and A. R. Lou. 2017. Impacts of the removal of shrubs on the physiological and biochemical characteristics of Syntrichia caninervis Mitt: In a temperate desert. *Scientific Reports* 7: 1–12.
Zanatta, F., R. Engler, F. Collart, O. Broennimann, R. G. Mateo, B. Papp, J. Muñoz, et al. 2020. Bryophytes are predicted to lag behind future climate change despite their high dispersal capacities. *Nature Communications* 11.
Zeileis, A., and T. Hothorn. 2002. Diagnostic Checking in Regression Relationships. *R News* 2: 7–10.
Zhang, F., J. A. Biederman, M. P. Dannenberg, D. Yan, S. C. Reed, and W. K. Smith. 2021. Five decades of observed daily precipitation reveal longer and more variable drought events across much of the western United States. *Geophysical Research Letters* 48: 1–11.
Zhang, J., and Y. Zhang. 2019. Ecophysiological responses of the biocrust moss *Syntrichia caninervis* to experimental snow cover manipulations in a temperate desert of central Asia. *Ecological Research* 35: 198–207.
Zhang, Y., X. Zhou, B. Yin, and A. Downing. 2016. Sensitivity of the xerophytic moss *Syntrichia caninervis* to prolonged simulated nitrogen deposition. *Annals of Botany* 117: 1153–1161.
Zhang, X., Y. Zhao, and S. Wang. 2017. Responses of antioxidant defense system of epilithic mosses to drought stress in karst rock desertified areas. Acta Geochimica 36: 205–212.

APPENDIX

Supplement 1. Microhabitat type relative frequency by life zone site
Relative frequency (proportion by site) of three microhabitat types (shrub proximity classes: canopy, dripline, interspace) supporting *Syntrichia caninervis* in the DNWR life zone sites. Surveying for microsite distribution was conducted within a 2-km radius of each life zone climate tower and should be representative of life zone patterns at large in the Mojave Desert.

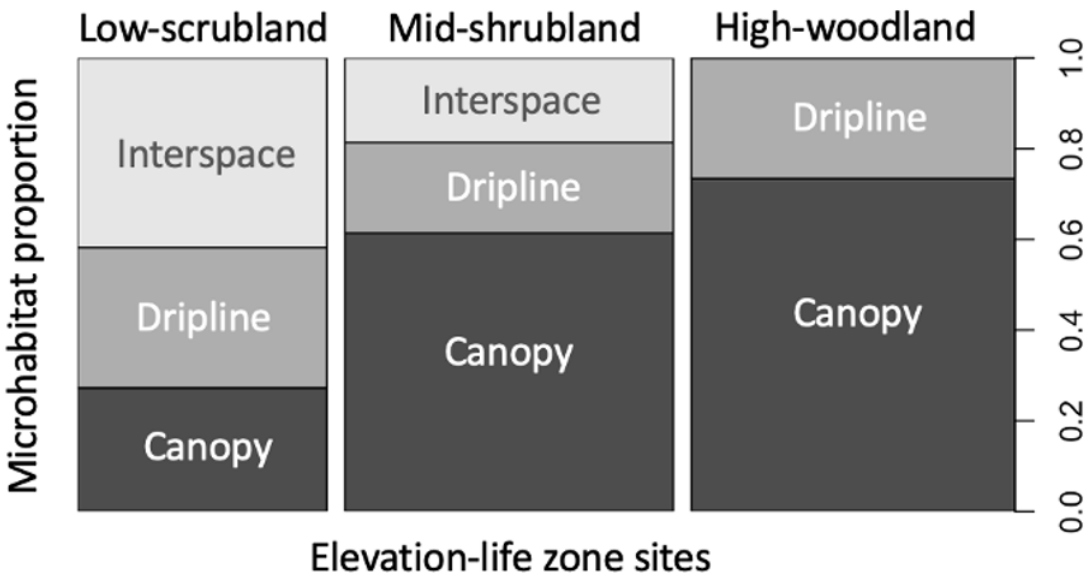

Supplement 2. Correlation and regression table for full habitat buffering model
A. Pearson's correlations table between regression predictors in the following models. **B**. Full OLS linear regression model of the relationship of summer moss stress (Fv/Fm) in *Syntrichia caninervis* and three habitat buffering proxies: life zone elevation (***Elevation***), potential direct incident radiation (***PDIR***), microscale shade time (***Shade.Index***), and their interactions. Elevation and shade suffer from multicollinearity such that this model is appropriate only for prediction rather than precise coefficient estimation (***see Analysis***). **C.** Corresponding ANOVA model (Type I errors) results, which do not suffer from multicollinearity; residual plots reasonably met assumptions and are not shown.

A

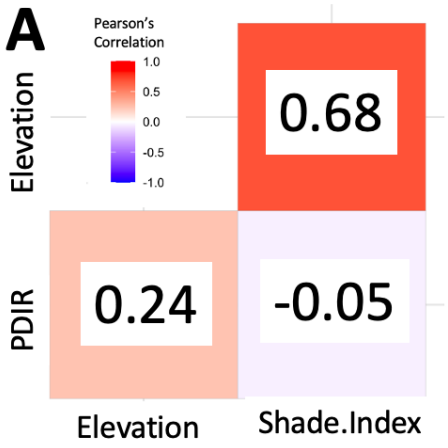

B **Full regression model coefficients & standard errors**

	Estimate	Std. Error
(Intercept)	0.29541280	1.68464416
Elevation	0.00191438	0.00141486
PDIR	0.27697979	1.77041616
Shade.Index	-0.02540937	0.09569381
Elevation:PDIR	-0.00231605	0.00147387
Elevation:Shade.Index	-0.00005336	0.00006671
PDIR:Shade.Index	0.02625171	0.10293684
Elevation:PDIR:Shade.Index	0.00006893	0.00007060

C **ANOVA Table**

	Df	Sum Sq	Mean Sq	F value	Pr(>F)	
Elevation	1	0.0402	0.0402	3.710	0.05747	.
PDIR	1	0.4068	0.4068	37.514	0.00000002808	***
Shade.Index	1	0.4585	0.4585	42.288	0.00000000536	***
Elevation:PDIR	1	0.0034	0.0034	0.314	0.57687	
Elevation:Shade.Index	1	0.1193	0.1193	11.006	0.00134	**
PDIR:Shade.Index	1	0.0956	0.0956	8.813	0.00390	**
Elevation:PDIR:Shade.Index	1	0.0103	0.0103	0.953	0.33172	
Residuals	84	0.9108	0.0108			

Signif. codes: 0 '***' 0.001 '**' 0.01 '*' 0.05 '.' 0.1 ' ' 1

Residual standard error: 0.1041 on 84 degrees of freedom
Multiple R-squared: 0.5546, Adjusted R-squared: 0.5175
F-statistic: 14.94 on 7 and 84 DF, p-value: 0.000000000001615

Supplement 3. Residual diagnostic plots for reduced habitat buffering regression model
Residual diagnostic plots (*R stats::plot(Y~X1*X2)*) for the OLS (ordinary least squares) regression model for moss stress (Fv/Fm) as a function of two habitat buffering predictors and their interaction term: potential direct incident radiation (PDIR) and annual shade time. See ***Analysis*** for details on model selection and **S2** for the full model. Model statistics and plot are in **Figure 7**.